UTS UNIVERSITY OF TECHNOLOGY SYDNEY

Enhancing the performance of lithium recovery in seawater with membrane distillation and manganese oxide metal-organic framework nanoparticles

by Sharaniya Roobavannan

Thesis submitted in fulfilment of the requirements for the degree of

Master of Engineering.

under the supervision of Prof. Saravanamuthu Vigneswaran and Dr. Gayathri Naidu

University of Technology Sydney
Faculty of Engineering and Information Technology

August 2021

Certificate of original authorship

I, Sharaniya Roobavannan declare that this thesis, is submitted in fulfilment of the requirements for the award of Master of Engineering, in the Faculty of Engineering and Information Technology at the University of Technology Sydney.

This thesis is wholly my own work unless otherwise referenced or acknowledged. In addition, I certify that all information sources and literature used are indicated in the thesis.

This document has not been submitted for qualifications at any other academic institution.
This research is supported by the Australian Government Research Training Program.

Production Note:
Signature removed prior to publication.

Signature of student
(Sharaniya Roobavannan)
Date: 13-08-2021

Acknowledgements

I would like to express my sincere gratitude to my principal supervisor Professor S. Vigneswaran and my co-supervisor, Dr. Gayathri Naidu, for their supervision, continuous guidance, encouragement, and support at all levels during my study at UTS.

In addition, I would like to thank Dr. Md Johir who has taught me how to use the analytical instruments in the UTS laboratory and Dr. Niren Pathak who has supported me in the laboratory analysis.

I am also thankful for the academic and technical support of the University of Technology Sydney and its staff. I appreciate the support of my friends Charith Fonseka, Alex Hienphuong and SeongChul Ryu at CTWW and all my friends in Sydney.

Finally, I wish to thank my husband Mahendran Roobavannan for his unconditional love and encouragement throughout the whole journey that he has taken with me. It would not have been possible without you. Furthermore, I would like to thank my father, my sisters and my loving son for their support and love.

Journal article published.

Roobavannan, S., Vigneswaran, S. & Naidu, G. 2020, 'Enhancing the performance of membrane distillation and ion-exchange manganese oxide for recovery of water and lithium from seawater', Chemical Engineering Journal, vol. 396, p. 125386.

LIST OF ABBREVIATIONS

SWRO	Sea Water Reverse Osmosis
DCMD	Direct Contact Membrane Distillation
MD	Membrane Distillation
HMO	Hydrogen Manganese Oxides
ZIF-8	Zeolitic Imidazolate Framework 8
MOF	Metal Organic Framework
LMO	Lithium Manganese Oxides
LIBs	Lithium-Ion Batteries
AGMD	Air Gap Membrane Distillation
VMD	Vacuum Membrane Distillation
SGMD	Sweeping Gas Membrane Distillation
MOFs	Metal-Organic Frameworks
PTFE	Polytetrafluoroethylene
Hmim	2-Methylimidazole
VCF	Volume Concentration Factor
ICP-MS	Inductively Coupled Plasma Mass Spectrometry
TDS	Total Dissolved Solids
LC-OCD	Liquid Chromatography with Organic Carbon Detection
SEM	Scanning Electron Microscope
EDS	Energy-Dispersive Spectroscopy
XRD	X-Ray Powder Diffraction
PFO	Pseudo First Order
PSO	Pseudo Second Order

CAPEX	Capital Expenditure
OPEX	Operational Expenditure

Contents

List of Figures

List of tables

Abstract

Growing population and climate change have significantly increased the demand for drinking water. Desalination plants are used to convert seawater into fresh drinking water using the reverse osmosis process. In sea water reverse osmosis (SWRO) process, water from a pressurized saline solution is separated from the dissolved salts by flowing through a water-permeable membrane. This process needs to dispose the waste containing concentrated brine. The concentrated brine from these plants contributes approximately 40% of their output and must be dealt immediately. Disposal of this waste directly into the sea has significant damage to the marine environment and it must be addressed. Conventional approaches to the problem presented by the concentrate involve treating the concentrate and then discharging the treated water into open water bodies or reusing it. However, these approaches typically have high operational costs, a necessity for large-scale operations, low productivity, and are chemically intensive. Consequently, an alternative approach is to adopt zero liquid discharge with resource recovery, generating additional revenue as well as protecting the environment.

Seawater contains economically valuable metals, such as Lithium (Li^+) but these are present at relatively low concentrations compared with Sodium (Na^+), Potassium (K^+), Calcium (Ca^{2+}) and Magnesium (Mg^{2+}) and are currently not recovered commercially. Recovering lithium (Li^+) from seawater is a sustainable alternative to meet its high demands. Li^+ recovery from seawater must be enhanced to attain economic efficiency.

In this work, the potential of enhancing Li^+ recovery from seawater is evaluated by firstly treating and concentrating seawater to produce fresh water while increasing Li^+ concentration using direct contact membrane distillation (DCMD) and reducing competitive ions; and thereafter to develop an efficient novel adsorbents, acid treated manganese oxide ion sieve (HMO) for converting waste brine from desalination plants into a desirable resource through extracting economically valuable lithium (Li^+)

Membrane Distillation (MD) ia an alternative membrane approach for treating concentrate. MD is a thermally driven membrane process based on mass transfer through a microporous hydrophobic membrane. The driving force is normally a temperature gradient between the heated side (feed) and cold side (permeate) of the membrane. The hydrophobic nature of the membrane prevents liquid intrusion into the pores, so only water vapour is transported through the membrane and condensed on the cooling side (permeate). MD has features that make it attractive for seawater concentrate treatment: (i) the low thermal requirement (45–60°C) allows

integration with alternative thermal sources such as solar, making it a sustainable process; (ii) it can produce high-quality fresh water suitable for reuse; (iii) it can concentrate seawater up to its saturation limit, reducing volume while increasing concentrations of valuable metals for selective recovery. In this study a lab scale direct contact membrane distillation (DCMD) was used to treat and concentrate seawater and pre-treated seawater (caustic soda ash and oxalic acid). DCMD performance with seawater and pre-treated seawater as feed solutions achieved an initial permeate fluxes of 25.5±0.8 L/m2h (LMH) with high quality permeate/freshwater characteristics (> 96% ion rejection). However, DCMD operated with seawater and caustic soda pre-treated seawater exhibited rapid decline of permeate fluxes (86-90%) by a volume concentration factor of 3 times onwards. Typically, seawater, in its original condition contain Ca2+ in the range of 350 - 400 mg/L. It is highly challenging for MD to treat original seawater due to the inevitable development of Ca^{2+} based scaling in thermal condition, namely, CaSO4. DCMD achieved enhanced water recovery upon pre-treatment with oxalic acid (88–91%) compared to caustic soda ash (65–68%) and without pre-treatment (47–51%). Caustic soda ash required Na+ addition in alkaline condition for Ca^{2+} removal, while oxalic acid removed Ca^{2+} in acidic condition without any inorganic ion addition. The low ion concentration in acidic condition upon oxalic acid pre-treatment enabled DCMD to concentrate seawater to high levels, increasing Li^{+} concentration by 7 times.

In Li^{+} solution, HMO achieved a maximum adsorptive capacity of 17.8 mg/g in alkaline condition. Multiple cycles of desorption and regeneration of HMO showed only 7–11% decline of Li^{+} uptake and minimal Mn dissolution, which, established HMO's reuse capacity. Selective Li^{+} mechanism is attributed to H/Li exchange as well as high negative surface charge of HMO. In seawater, Li^{+} uptake by HMO reduced by 44–46% due to the presence of Mg^{2+}. Seawater with minimal Mg^{2+} was favourable for enhancing Li+ uptake by HMO. Seawater treatment in stages – divalent pre-treatment and concentrating seawater, followed by HMO, provided a favourable scenario for attaining high.

quality water, selective Li^{+} recovery, and other resources – Ca^{2+} and Mg^{2+}. The drawback of this method is HMO can only recover Li at high pH (11-12). Therefore, in this study, a new HMO with metal organic framework -ZIF-8@MOF was synthesised for the first time. The ZIF-8@MOF showed higher Li+ adsorption capacity compared to HMO. More importantly, ZIF-8@MOF can selectively extract Li^{+} in seawater at its original pH (7.5-8.0). This is favourable in attaining selectively Li^{+} recovery from seawater without the need for pH adjustment to 11 with chemical addition (NaOH).

CHAPTER 1

INTRODUCTION

1. Introduction.

1.1. Background of research

Seawater is a complex solution comprising of a vast variety of elements. Apart from major ions in high concentration such as Na^+, Mg^{2+}, Ca^{2+} and K^+, seawater also contain valuable trace elements that are scarce in mine ores such as Rb and economically important Li^+ (Flexer et al., 2018, Loganathan et al., 2017). The interest of recovering Li^+ from natural sources is attributed to its rising demand as high energy storage battery (Flexer et al., 2018, Grosjean et al., 2012). Given the amount of seawater is extensive and inexhaustible, the total Li^+ in seawater is projected to be much larger than that of mine-ores. Globally, over 200 Gt mass of Li^+ could be extracted from seawater. Further, compared to Li^+ extraction from mine ores (which involves complex hydrometallurgical processes with high chemical usage), extraction of Li^+ from seawater is less detrimental towards the environment (Flexer et al., 2018, Meshram et al., 2014, Naidu et al., 2020). Due to these factors, the recovery of valuable Li^+ from seawater is becoming an attractive option. Several methods have been evaluated for Li^+ recovery from seawater such as evaporation/precipitation, selective membrane processes, electrodialysis, electrochemical and ion exchange adsorption (Flexer et al., 2018, Li et al., 2019, Loganathan et al., 2017, Meshram et al., 2014). For instance, membrane technologies such as pressure driven nanofiltration, supported liquid Membrane and electrically driven membrane-based technologies namely electrodialysis and capacitive deionization with selective exchange membranes are being applied for Li^+ extraction (Li et al., 2019). Positively charged nanofiltration membranes have been effective for selective Li^+ separation(from Mg^{2+})from brine (Zhang et al., 2017). Likewise, supported liquid Membrane with solvent exchange enables to attain selective Li^+. However, the main challenges of Li^+ extraction by membrane process such as nanofiltration is membrane fouling during brine treatment while stability and solvent leakage remains challenges of liquid membranes. Comparatively ion exchange adsorption is widely adopted due to its capacity to selectively extract Li^+ present in trace concentration from complex seawater solution at a relatively low cost with ease of operation for practical industrial application. Specifically, inorganic lithium manganese ion sieves synthesised from lithium manganese oxides (LMOs), such as $Li_{1.6}Mn_{1.6}O_4$, $LiMn_2O_4$, and $Li_{1.33}Mn_{1.6}7O_4$, display excellent performance for selective uptake of Li^+ from seawater (Chitrakar et al., 2001, Feng et al., 1992, Nishihama et al., 2011, Ryu et al., 2019, Tian et al., 2010). The high selective Li^+ capacity of LMOs is attributed to its unique topotactic Li/H ion exchange characteristics that extract Li^+ in LMO by ion exchange with H^+ when treated in

acidic solution, producing H-form manganese ion sieves (HMO). Further, HMO consists of pore sizes similar to that of Li ion compared to other ions in seawater, which allows for selective Li^+ uptake. Li^+ uptake from seawater and saline brine using various types of HMO has been reported by previous studies. For instance, Wang et al. (Wang et al., 2020) synthetized three types of HMO using furnace and hydrothermal method and reported the capacity of HMO to selectively extract Li^+ from geothermal brine. In another study, Gu et al. (2018) used an improved solid-state method to synthesis lithium-ion sieve with titanium and achieved enhanced Li^+ uptake from Salt Lake brine. Liu et al.(2015) used sol-gel and hydrothermal method to synthesize spinel manganese oxide ion sieve with one-dimensional nanowires for Li^+ extraction from seawater.

However, despite HMO's capacity for selective Li^+ uptake in seawater, this ion exchange adsorption approach is unable to attain economic efficient Li^+ recovery from seawater. One of the primary reasons for this is the low concentration range of Li^+ (0.14–0.19 mg/L) in seawater. It is well-established that the initial concentration of ions plays a significant role in influencing the performance capacity of adsorbents (Hong et al., 2013, Tian et al., 2010). Concentrating seawater, in effect, will enable to increase initial Li^+ concentration, thereby, enhancing the capacity of HMO. Thus far, previous studies have evaluated this phenomenon by spiking higher Li^+concentration in model solution as well as in mixed solutions such as seawater brine (Liu et al., 2015, Park et al., 2014, Tian et al., 2010). For instance, Tian et al.(Tian et al., 2010) achieved 75% higher Li^+ uptake with HMO by spiking the initial Li^+ concentration in a model solution from 20 mg/L to 35 mg/L. Compared to previous studies, for the first time, this study investigated the potential of increasing Li^+ concentration in actual seawater by treating/concentrating seawater while simultaneously producing fresh water using membrane distillation (MD).

Membrane distillation (MD) offers the potential to concentrate seawater (in turn, increase Li^+ concentration) while producing reusable freshwater. As a thermal vapour pressure driven process using a hydrophobic membrane, MD is not significantly affected by high salinity. Hence, compared to seawater desalination with reverse osmosis, MD in principle, can achieve highly concentrated seawater while producing good quality fresh water. The potential of MD as an alternative seawater desalination treatment process has been successfully demonstrated by a number of researchers (Winter et al., 2011, González et al., 2017, Mericq et al., 2010). Although MD can effectively treat seawater, in thermal condition, inorganic Membrane scaling, specifically, $CaSO_4$ deposition onto the Membrane, is a major phenomenon that

compromises the capacity of MD to achieve high water recovery while concentrating seawater (Choi et al., 2017, Lee et al., 2018). Minimizing Ca^{2+} content (seawater softening) is a practical approach to control CaSO4 scaling in MD. In line with this, Li et al. (Li et al., 2019) indicated the importance of minimizing membrane scaling and fouling to enhance the efficiency of membrane processes such as nanofiltration and MD for treating and concentrating Li^{+} from brine.

A conventional chemical method adopted for water softening (divalent removal) is caustic soda ash addition (Sanmartino et al., 2017, Semblante et al., 2018, Sorour et al., 2015). A few MD studies for seawater brine treatment have demonstrated improved MD performance with caustic soda softened brine (Sanmartino et al., 2017, Ji et al., 2010, Kim et al., 2020). For instance, Sanmartino et al. (Sanmartino et al., 2017) demonstrated the capacity of MD to concentrate caustic soda ash softened seawater brine from 55 g/L by up to 350 g/L.

Comparatively, without caustic soda ash softening, seawater brine was only concentrated up to 153 g/L. Likewise, Ji, et al. (Ji et al., 2010) used caustic soda ash softening in seawater brine to reduce scaling and to obtain higher brine concentration levels in MD-crystallizer. Nevertheless, it is still a challenge for MD to achieve highly concentrated seawater levels with caustic soda ash softening. This is because Ca^{2+} precipitation in caustic soda ash approach occur in alkaline condition, thereby, requiring the addition of sodium hydroxide to increase seawater pH. The addition of sodium (from hydroxide and carbonate) increases ion concentration in seawater. Invariably, ion concentration effect becomes more prevalent, especially as MD attempts to continuously concentrate the seawater, resulting in permeate flux decline over time (Guan et al., 2018, Eykens et al., 2016). Further, the residues of hydroxide and carbonate in alkaline thermal condition, increases susceptibility towards scale formation onto the membrane, which invariably compromises the capacity of MD to further concentrate seawater (Qu et al., 2009).

In comparison to caustic soda ash softening, organic Poly carboxylic acids such as oxalic acid may offer an alternative approach to seawater softening without the addition of sodium. The high catalytic capacity of oxalic acid has been demonstrated for hydrolysing biomass (Lee et al., 2013), mineral surface dissolution (Salmani Nuri et al., 2019), acidification for sewage sludge dewatering (Chen et al., 2020) and fermentation of algae (Knoshaug et al., 2018). In the field of hydrometallurgy, oxalic acid demonstrated superior scalant mitigation capacity compared to caustic soda ash, due to its capacity to selectively precipitate Ca^{2+} without any

additional ions (sodium/hydroxide/carbonate) introduced to the solution. Further, oxalic acid exhibits capacity for selective Ca^{2+} removal in mixed solutions containing both Ca^{2+} and Mg^{2+} (Moldoveanu and Papangelakis, 2015). On this basis, oxalic acid could be suitable to attain selective Ca^{2+} removal from seawater without introducing any additional ions, and thereby, minimizing scaling during MD process. Further, unlike the alkaline condition of caustic soda ash, the acidic condition with oxalic acid could be beneficial to increase induction time of saturated ion, in turn, delaying precipitation of ions (Gryta, 2010). The suitability of oxalic acid as a seawater pre-treatment for scaling mitigation in MD is yet to be explored. For the first time, this study compares the effectiveness of caustic soda ash over oxalic acid as Ca^{2+}removal method from seawater. Further, upon MD treatment, the capacity of oxalic acid treated seawater to retain Li^{+} mass with minimal losses through co-precipitation must be evaluated. Detailed investigation is necessary to establish these scenarios.

1.2. Objective of this research.

Growing population and climate change have significantly increased the demand for drinking water. Seawater is not suitable for drinking. Because the salt concentration is high. Desalinations is a one of technology is used to satisfy the water demand. Therefore, recently many desalination plants are established in the world to produce drinking water. Mainly they are using seawater reverse osmosis (SWRO) technology. So this technology, convert seawater into fresh drinking water and seawater brine. But a major problem of this process is, they need to dispose the concentrated brine immediately. But These plants do not have specific brine management process. Disposal of the concentrate brine on land will cause pollution to surface water and groundwater. So, the alternative solution is converting this seawater brine in to use full by-product.

Seawater is a complex solution containing of a vast variety of elements. The major ions are Na, Mg, Ca and K. and also seawater contains economically valuable elements, such as Strontium (Sr), Lithium (Li), and Rubidium but these are present at relatively low concentrations compared with major elements and these are currently not much recovered for the commercial purpose. Lithium is consumed in a wide range for the largest researchable battery production market. Now a days the world market mainly focuses on electric cars. Apart from batteries, lithium is essential for applications in glass and ceramics, greases and chemicals/pharmaceuticals industries. The Li_2CO_3 requirement in 2025 is estimated to be 498 kilo tons, it is compared to be very high from past years.

But Lithium recourse is very limited in land, so the good alternative option is recovering the Li ions from the waste seawater brine.

The aims of this study are to examine the performance of HMO for Li^+ uptake from seawater and identify favourable conditions to enhance the capacity of HMO for selective Li^+ uptake. For these reasons,

I. Concentrate Li in seawater.

The potential of DCMD to achieve high water recovery while increasing Li^+ concentration in seawater upon chemical softening was evaluated. Specifically, the suitability of oxalic acid compared to caustic soda ash as a seawater chemical softening agent for mitigating scaling in DCMD was examined.

II. **Selective Li recovery with manganese oxide from seawater.**

To understand the mechanisms of selective Li^+ uptake of HMO and identify conditions that enhances its performance, detailed chemical and physical characteristics of HMO was analysed. Factors that influence HMO performance such as pH, surface charge, time, equilibrium dose and concentration was evaluated. Further, the role of ion competition was examined by comparing HMO performance for selective Li^+ uptake in original seawater and pre-treated concentrated seawater. Lastly, desorption and regeneration of HMO was carried out to establish the reusable capacity of HMO.

III. Enhancing Li recovery with manganese oxide metal organic framework nanoparticles.

Finally, to increase the surface area of nanoparticle, the HMO adsorbent was combined with a porous metal−organic framework (MOF) and the adsorbent provide functional groups for increased selective Li^+ extraction at pH of 8 (seawater pH) to extract the lithium from seawater.

CHAPTER 2

LITERATURE REVIEW

2. Literature review

2.1. Introduction

Water desalination, a significant source of water production, utilizes seawater to produce freshwater. The process is energy-intensive and generates large amounts of concentrated brine, which are treated as waste and often disposed into surface waters. By improving the existing infrastructure of water desalination plants, the management of seawater and brine concentrate can be enhanced to produce more freshwater and valuable minerals and energy. Seawater and concentrated brine contain valuable resources that can be recovered, potentially leading to profit and reduced waste disposal. With the recent developments in membrane-based technologies, increased water production and natural resource recovery from brine and seawater are now feasible or have improved. This step toward zero-liquid discharge not only relieves some of the stress regarding water scarcity but also reduces water pollution from waste disposal.

Changes in the infrastructure of water desalination plants for the recovery of marketable minerals from brine concentrate, which is generally considered a waste stream, can provide a new avenue for sustainable mineral production. In contrast, current methods of resource production are expensive and unsustainable as a long-term strategy. For instance, lithium is a valuable mineral used in batteries since it is lightweight and has a high energy density. However, lithium production at mining sites is struggling to keep pace with the growth in lithium demand (Alsabah et al.). As the resources at mining sites grow scarcer, mining operations require more significant amounts of water, leading to economic and environmental burdens. By investigating and implementing technologies for brine treatment, valuable minerals such as lithium can be recovered from brine and effectively reduce the volume of discharged waste.

The recovery of resources from waste streams is a crucial aspect of sustainable future societies. Specifically, given the current widespread concerns for climate change and rising resource prices, moving from a linear economic model (i.e., “take-make-dispose”) to a more circular or closed-cycle model (e.g., “take-make-revalorize-reuse”) is gaining traction as an achievable policy goal (Gregson et al., 2015). In the field of seawater desalination, today’s approach focuses only on what must be removed (i.e., metals from seawater) without considering the process byproducts as resources themselves (Guest et al., 2009). Extractable resources from seawater can be grouped into three macro-categories: water recovery, energy recovery, and resource recovery. Technologies have been devised for extracting metal resources from the

water present in the form of concentrated solutions. These technologies can be used to recover resources from wastewater effluent, except that they are present at low concentrations, and hence their extraction may be economically less viable. Any liquid waste generated following specific intended anthropogenic uses is termed wastewater and can include wastewater produced from industries, mining activities, domestic water use,. Depending on the wastewater sources, the types of resources that can be recovered and their concentrations could vary, although similar technologies can be used depending on the target resources.

Focused on in this study are resource recovery of valuable lithium from seawater and its related brine from desalination treatment.

2.2 Resource recovery from seawater and its related brine

Oceans and seas contain 96.7% (1.3×10^{18} tons) of water, while dissolved salts amount to 3.3% (5×10^{16} tons) (Loganathan et al., 2017, Ryu et al., 2019). The oceans comprise massive quantities of dissolved ions. Virtually every element in the periodic table can be detected in seawater, although several elements exist at minimal concentrations. According to Loganathan et al. (2017) and Li et al. (2019), the key ions making up 99.9% of the salts in seawater in decreasing order are as follows: Na+ > Mg^{2+} > Ca^{2+}, K^+ (for cations) and Cl^- > SO4 $^{2-}$ > HCO_3^- > Br^- > BO_3^{2-} > F^- (for anions). Ever since ancient times, minerals have been extracted from seawater, and one typical example is sodium chloride, otherwise known as normal table salt (Ryu et al., 2019). This research currently considers only group I and group II periodic table elements, which are positive ions dissolved in seawater. The four most concentrated metal ions - $Mg2^+$, Na^+, K^+, and Ca^{2+}, are currently the only industrially ones that are being extracted (Ryu et al., 2019, Zhang et al. 2021).

Several factors determine the feasibility of recovering an element from source water. These are (i) extraction efficiency, (ii) concentration of elements in the source water, and (iii) the economic value (market price) working in tandem with the economic significance (industry demand) of a resource. When categorizing elements based on economic value over economic importance (**Fig. 1**), only a few elements fall under the feasible recovery matrix (economic importance more than 5; economical price more than1). For example, silver, uranium, rubidium, and gold possess high economic value (market price), according to Loganathan et al. (2017); however, their economic importance (ranking level of less than 5) is minor, given that these elements do not have a broad industry purpose. Conversely, an element like lithium does have both economic value and economic importance, given the surging industrial demand

for lithium batteries (Flexer et al., 2018). Furthermore, according to Ober (2018), the as-yet small global lithium production (see Fig. 1 below) means that it ranks high on the economic vulnerability scale.

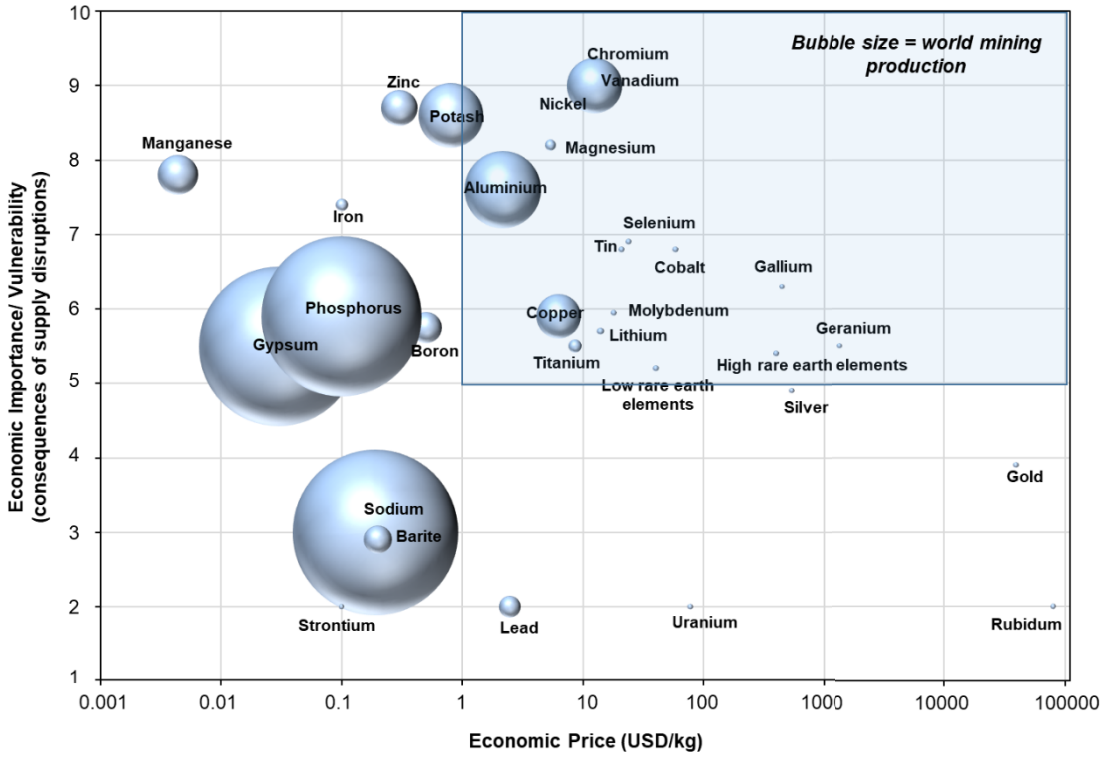

Figure 1: 3D matrix representation of viable resource recovery ranking on the basis of economic price of resources (in USD/kg) and economic vulnerability/importance (bubble size of each resource represents global mining output (based on the summary of USGS2018 mineral commodities) (Ober, 2018); resource pricing/value extracted from EU ranking (Glöser et al., 2015).

2.3 The demand for lithium

Lithium exists as the earth's 25th most abundant element (at 20 mg/kg) (Meshram et al., 2014), and the lightest alkali metal of all, having a density of 0.534 g/cm^3 (W.A. Hart, 1973, Choubey et al., 2016). It is important to note that lithium is electrochemically active, with firstly, it has a high electrode potential of −3.05 V; secondly, the highest specific heat capacity of any solid element (W.A. Hart, 1973, Choubey et al., 2016). With these properties, lithium compounds are desirable in many commercial applications, and the global distribution of lithium end-uses in various applications was documented in 2016 (Flexer et al., 2018). Lithium has been employed in the manufacture of glass and ceramic materials, aluminum, types of grease, and other materials (Flexer et al., 2018).

In the last decades years, demand for lithium has hugely increased because it is a vital component of the lithium battery. According to one EU report, lithium extraction overrides the threshold level due to the commercial importance attached to it, and it is very close to the supply risk threshold (Flexer et al., 2018).

Lithium is an integral part of rechargeable lithium-ion batteries (LIBs) because it is characterized by excessive energy density according to weight and high electrochemical potential (3.045 V). The current consumption level is nearly twenty-two percent of the total lithium produced in LIBs, and by 2020 it is expected that this will reach almost forty percentage (Wang et al., 2012). Apart from batteries, lithium at present has essential applications in glass and ceramics (30%), metallurgical industries (4%), greases (11%), chemicals/pharmaceuticals, rubber-derived materials. (Holdren, 1971, Granata et al., 2012). It was stated in the now-decade old Madrid Report of July 2010 that lithium straddles the border line of low-to-medium supply and demand, and Meshram et al. (2014) have contended this is primarily due to insufficient resources. Furthermore, the need for lithium is rising further because it has nuclear power and related strategic uses. A recent study on the reserves of lithium has estimated that from around 100 deposits containing over 1,00,000 tons lithium, the lithium reserves of every deposit differ and have unique mineral properties. As a result, specific technologies must be used for processing different mineral properties, in order for the process to be cost effective (Gruber et al., 2011). Due to this factor, generally, lithium extraction is only carried out from selective mine ores (predominantly spodumene) as well as LiCl salts from brine lake/pools. (Meshram et al., 2014).

Constant and robust growth in the demand for lithium is expected to continue well into the future, made possible by the various forms of lithium batteries. These constitute the most promising entrants for powering hybrid vehicles and generating electricity (Opitz et al., 2017). These batteries include both existing technologies, for instance, lithium-ion, and emerging battery technologies like lithium-sulfur or lithium-air (Winter and Brodd, 2004). The public mainly associates lithium batteries with portable electronics and electric and hybrid vehicles. In contrast, high-capacity lithium batteries have emerged as a possible, solid solution for storing energy for the electrical power grid, i.e., smart grids. Large capacity batteries are urgently required to accumulate green types of energy, i.e., solar, waves, and wind and waves. These are created in the natural world, but they are also intermittent energy sources (Brouwer et al., 2016), so this is a problematic scenario when consistent energy needs to be delivered.

Moreover, many industries require large amounts of lithium salts, which to date add up to approximately 65% of the world's lithium demand. These enterprisers are also expected to keep growing, albeit at a slower pace, as the world's population continues to climb (Flexer et al., 2018). Although lithium contents in geothermal brine is reasonably high (up to 20 mg/L) (Shahmansouri et al., 2015), these brines tend to also contain other metals in significantly higher concentrations, namely, arsenic, boron, and mercury, attributed to the contact between the heated water (underground) and stones/rocks (Siekierka et al., 2018). Comparatively, lithium contents in natural Salt Lake brine can range between hundreds to thousands of parts per million. The challenge here is to selectively extract lithium over competing/interfering ions, specifically magnesium, by which, the Mg^{+}/Li^{+} ratio is around 40 and sometimes in extreme cases can be up to 200 (Song et al., 2017). Due to the unique chemical combination of natural water-based lithium resources, the selective recovery of lithium from water-based sources is still a challenge. Even though the overall mass of Li^{+} available in these natural water sources are promising, the high concentration of interfering ions remains a significant problem for attaining a sustainable lithium extraction. (Flexer et al., 2018).

Australia is currently one of the world's top Li^{+} producers, and the source is land mining (Flexer et al., 2018, Gray, 2018). The rapid rise in the demand for lithium (Li^{+}) is due to its importance as a primary ingredient in Lithium batteries. Lithium batteries are used to power electric or hybrid vehicles, electronic devices but are now considered a prime candidate for storing energy Meshram et al., 2014; Loganathan et al., 2017; Flexer et al., 2018). The current Li^{+} demand (average 265-kilo tons in 2015) is projected to rise by 90% in 2025 (estimated 498-kilo tons) (Meshram et al., 2014, Flexer et al., 2018, U.S. Geological Survey, 2018). Industries and governments worldwide — and especially the projections made by the EU — believe that Li^{+} has passed the threshold for economic importance and is now very close to the supply risk threshold.

A consequence of having much more demand for Li^{+} is its economical price increment (USD13.9/kg of Li_2CO_3 in 2018) (U.S. Geological Survey, 2018). Invariably, Li's high demand correlates to an increasing dependence on Li^{+}mining and ore processing. For instance, seven new ore mines for Li^{+} production are now operating in Western Australia. Australia is projected to be one of the top global lithium suppliers, which was predicted decades ago by Holdren (1971).

The process of extracting Li^+ from rock mines requires the exploitation of large land areas, is chemical and energy-intensive, has high operating costs, and requires large volumes of water. Further, this temporary endeavour will inevitably result in long-term abandoned mines that are highly contaminated and will require expensive remediation at some point. It is subsequently critical to reducing the environmental pollution risks of our reliance on non-renewable land mining for Lithium. An alternative renewable Li^+ source with sustainable extraction features must be developed.

2.4 Seawater and its related brine as an alternative lithium source.

Environmental contamination and economic concerns concerning non-renewable rock mining have led to much research concentrating on alternative sources for lithium supply. For instance, research on the recycling of lithium batteries has accelerated in recent times. However, given the low concentration of lithium extraction from recycling, it has yet to attain economic viability compared to raw material mining (Flexer et al., 2018). Therefore, rather than rock, a potential alternative source of lithium is brine. Brine is attractive as an alternative source of lithium for the following reasons:

- Total lithium in brine is projected to be much larger than what exists in mine ores (Meshram et al., 2014, U.S. Geological Survey, 2018). Lithium concentration in brine sources can be as small as 0.2 mg/L, such as seawater (see **Table 1**). However, the amount of available seawater is extensive and inexhaustible. Globally, over 200 Gt mass of Li^+ could be recovered from it (Meshram et al., 2014, Luo et al., 2016, U.S. Geological Survey, 2018).
- Lithium extraction revenue could potentially offset the costs that arise from the need to treat brine produced industrially.
- Extraction of lithium from brine would not cause detrimental environmental contamination.
- Compared to the cost of extracting lithium from mine rocks (complex hydrometallurgical processes), lithium extraction from lithium-rich brines is expected to be substantially lower, especially with an efficient method.

Table 1. Concentration of major ions in brine and their characteristics.

Metal ions	Concentration in seawater (mg/L)[9]	Ionic radius, Å[10]	Electronegativity Scale χ [11]	Hydration enthalpy (kJ/mol)[8]
Na^+	27,500-30,000	1.02	0.93	-405
Mg^{2+}	1800-2450	0.72	1.31	-1922
Ca^{2+}	800-850	1.00	1.00	-1592
K^+	650-700	1.38	0.82	-312
Li^+	0.21-0.27	0.76	0.98	-515

2.5 Methods for lithium recovery from seawater and brine

Besides economic factors and source water identification, making resource recovery viable greatly relies on an appropriate method, given that seawater is a complex solution containing mixed components of varied elements. It is challenging to recover valuable elements such as lithium from seawater because separating the targeted element from another dominating ion is problematic. Several strategies have been devised for lithium recovery:

- ***Solar evaporation with crystallizer*** is a commercially adopted method for extracting lithium from salt lakes in South America and China. Although inexpensive, the process is prolonged (12-24 months) and relatively inefficient (Flexer et al., 2018).
- ***Liquid-liquid extraction organic solvents*** have been proposed as a Li extraction method (Shi et al., 2014, Flexer et al., 2018). However, this technique is poorly suited for large-scale implementation and results in chemical contamination.
- ***Nanofiltration*** with a small membrane pore size and hydraulic pressure is suited for separating Li^+ from divalent ions and mostly Mg^{2+}. However, it does not possess monovalent selectivity, and its practicality is hindered by brine's high salinity and scaling (Razmjou et al., 2019).
- ***Electrochemical-***driven technology, for instance, electrodialysis and capacitive deionization with ion-exchange membranes, are promising methods for selective Li^+ extraction under electric field due to its low energy and chemical

requirement, rapid, particular capacity in saline brine, and minimal byproduct contaminants (Choi et al., 2019, Razmjou et al., 2019).

- ***Adsorption*** is widely used for Li^+ extraction due to its comparatively low cost, simplicity of setup, efficient selective capacity over competitive ions, and ease of operation (Flexer et al., 2018, Razmjou et al., 2019).

2.6 Adsorption

Adsorbents are a well-established and straightforward approach to selectively extract valuable low concentration metals using the adsorption/desorption process. Adsorption is defined as the accumulation of a substance at the interface between two phases: solid and gas or solid and liquid. A sense accumulating at the interface is called an 'adsorbate.' At the same time, the concrete on which adsorption occurs is an 'adsorbent.' The adsorbents used for extracting metals can take the form of chelating resins and nanomaterials, organic polymeric ion exchange resin, or inorganic compounds. Selective adsorption of metals by adsorbent is guided by ligand exchange, inner-sphere complexation, or specific adsorption, which incorporates ion exchanging with ion within the adsorbents' crystal lattices.

In some cases, the surface of the ion exchange adsorbent contains unbalanced forces of attraction responsible for adsorption (electrostatic attraction). In scenarios where adsorption is due to weak van der Waals forces, this is termed physical adsorption (outer-sphere complexation). In contrast, chemical ion exchange mechanisms between adsorbent and adsorbate molecules are referred to as chemisorption (Dabrowski, 2001, Bhatnagar and Sillanpää, 2010). To quote Chitrakar et al. (2001), "the adsorption process is appropriate for extraction of lithium from seawater brine since certain inorganic ion-exchange materials display high selectivity for lithium ions only." In the last 20 years, many studies have been published on lithium adsorption from seawater and seawater brine using various types of inorganic adsorbents (Chitrakar et al., 2001).

2.7 Adsorbent comparison.

Table 2: ion-exchange manganese oxide adsorbent comparison with other Lithium adsorbent studies.

Adsorbent	pH	Adsorption capacity (mg/g)	Competing metal/Ions	Ref
Li^+-IIP-Fe3O4@C	7.5	22.26	Na^+ K^+ Mg^{2+}	(Liang et al., 2020)
1-D MnO2	10.10	46.34	Na^+ K^+ Mg^{2+} Ca^{2+}	(Zhang et al., 2009)
iron-doped titanium lithium ion	8.8	39.8	Na^+ K^+ Mg^{2+}	(Wang et al., 2018)
Yolk-shell structured composite	10.2	6.65	Na^+ K^+ Mg^{2+} Ca^{2+}	(Li et al., 2018)

2.8. Lithium recovery from seawater and brine with manganese oxide ion-exchange adsorption

Numerous Li-ion sieve nanoparticles exhibit a high affinity for selective Li^+ extraction (Han et al., 2012, Luo et al., 2016, Loganathan et al., 2017). Here the inorganic adsorbents, spinel-type hydrous manganese oxides, have extremely high affinity to lithium ions only (Chitrakar et al., 2001). The spinel-type manganese oxide MnO_2 $.0.31H_2O$ is generally used as a lithium selective adsorbent because: firstly, it retains high chemical stability against lithium insertion extraction in the aqueous phase (Ryu et al., 2016); and secondly, lithium uptakes were high (34-40 mg/g). This is despite the uptakes of other metal ions being low, i.e., <10 mg/g (Chitrakar et al., 2001).

Ion-sieve adsorbent is a kind of inorganic material in which the template ions are introduced into an inorganic compound by redox or ion exchange reaction, and a heating process obtains the compound oxide (Weng et al., 2020). A vital feature of the Li-ion sieve is that the spinel phase with Li-ion is located at the tetrahedral sites and manganese ions at the octahedral sites of the cubic close-packed oxygen framework (**Fig. 2**). Due to the oxygen framework, the Li-ion sieve reveals a negatively charged surface, resulting in electrostatic attraction towards positively charged cations. Because of the spinel structure, the Li-ion sieve can maintain Li ion-sized holes and selectively adsorb Li-ions through ion exchange with H ions. Li-ions with a small ionic radius can enter the spinel structure after dehydration. In contrast, other significant ions in brine (Na^+, K^+, Ca^{2+}) cannot do so due to their sizeable ionic radius **Table 1**). Furthermore, Li^+ can be easily extracted/desorbed from these adsorbents using hydrochloric acid (HCl), producing pure LiCl.

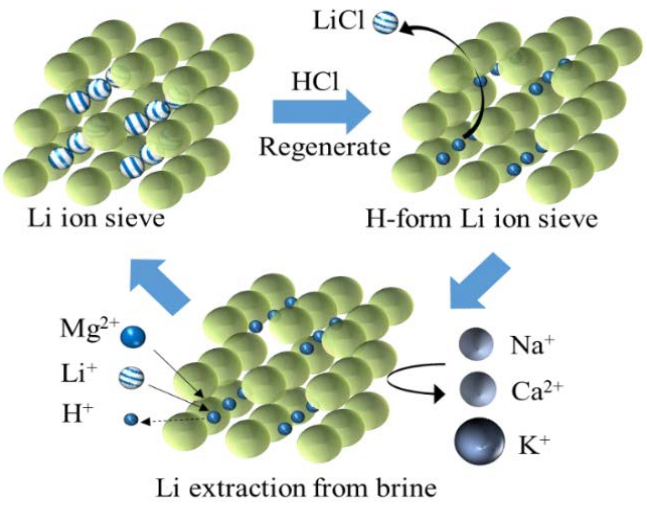

Figure 2. Selective Li^+ extraction and regeneration by H-form Li-ion sieve.

$$2(Li)[Mn^{3+}Mn^{4+}]O_4 + 4H^+ \rightarrow 1.5[\lambda Mn_2^{4+}]O_4 + 2Li^+ + Mn^{2+} + 2H_2O \quad (1)$$

$$Li_{1.33}Mn_{1.67}^{4+}O_4 + 1.33H^+ \rightarrow H_{1.33}Mn_{1.64}^{4+}O_4 + 1.33Li^+ \quad (2)$$

$$Li_{1.6}Mn_{1.6}^{4+}O_4 + 1.6H^+ \rightarrow H_{1.6}Mn_{1.6}^{4+}O_4 + 1.6Li^+ \quad (3)$$

Adsorbent materials contain the Li ion-sieve manganese oxides originating from lithium manganese oxides (LMOs), for example, $LiMn_2O_4$, $Li_{1.33}Mn_{1.64}O_4$, and $Li_{1.6}Mn_{1.6}O_4$. These are characterized by having high selectivity for Li^+, chemical stability, non-toxic nature, and low cost (Chitrakar et al., 2001, Tian et al., 2010, Ryu et al., 2019). While LMO demonstrates excellent adsorption performance, the inherent problem is that manganese ions are lost during Li^+ extraction from the adsorbent by acidic treatment. This is explained by an unstable spinel structure. Specifically, LMO is treated using an acidic solution so that Li^+ can be extracted by ion exchange before Li^+ adsorption. However, this process work should not interrupt the Li^+-free spinel structure, in the same way as explained in more detail below (Ryu et al., 2019).

2.9 Enhancing lithium recovery.

2.9.1 Concentrating lithium.

2.9.1.1 Membrane Distillation (MD).

Membrane distillation (MD) is an integrated heat-membrane filter separation system. Essentially, MD operates based on the principle of molecular distillation with vapor separation

through a micro-pored membrane with a hydrophobic surface (El-Bourawi et al., 2006, Criscuoli et al., 2013).The water movement/flux through the feed and permeate side pf the membrane is predominantly described by both mass and heat transfer mechanism (El-Bourawi et al., 2006, Khayet, 2011). The permeate condition influences the vapor/distillation driving force (El-Bourawi et al., 2006, Criscuoli et al., 2013). The main conditions on the permeate side that categorizes MD set-up are (i) AGMD - air gap membrane distillation, whereby, stagnant air is integrated into the permeate membrane side primarily with cold inserted plate ; (ii) DCMD - direct contact membrane distillation, whereby, cold solution/water is continuously flowed across the permeate membrane side; (iii) VMD - vacuum membrane distillation, whereby vacuum flow is continuously supplied to the permeate membrane side; (iv) SGMD - sweeping gas membrane distillation, whereby, gas is incorporated to the permeate membrane side (Naidu et al., 2020).

MD can reach significantly high (up to 99%) level/rate of salts/ions, colloids, organics, and emerging pollutants/contaminants. MD's capacity to treat and concentrate saline/hypersaline solution/wastewater, it is highly proficient, and this is attributable to its driving mechanics (vapor separation pressure). It is very much unlike membrane systems driven by applied pressure, for example, reverse osmosis and nanofiltration (Naidu et al., 2020). MD can concentrate seawater and seawater brine to high levels, which will shrink the volume of brine disposal (Naidu et al., 2020).

2.9.1.2 Direct Contact MD (DCMD)

Direct Contact membrane distillation (DCMD) is a thermal integrated membrane process driven by a vapor pressure gradient across a hydrophobic and microporous membrane (Warsinger et al., 2015). A feed stream and a receiving phase having a lower temperature are separated by the Membrane (Ashoor et al., 2016). What drives the force of heat transport is the temperature gradient across the Membrane, creating a water vapor pressure differential that causes water vapor to be transported through the membrane pores (Ashoor et al., 2016). The main competitive advantage of M.D. is that distillation happens below the feed solution's average boiling point. This separation method is based on the Equilibrium between the liquid molecules and the liquid mixture's vapor (Camacho et al., 2013). Working as a phase separation process, MD produces high-quality permeate (distillate) with a good amount being recovered because it is insensitive to a highly saline solution's osmotic pressure (Warsinger et al., 2015).

The molar water flux n_w can be described in the form of the following equation with an overall mass transfer coefficient C:

$$\dot{n}_w = C\,\Delta p_{\text{mem}} = C(p_1 - p_0) = C\frac{dp}{dT}(T_1 - T_0),$$

where p_1 and p_0 are, respectively, the vapor pressures at the hot feed water–membrane interface and the cold distillate–membrane interface. Mass transfer is based on the superposition of molecular diffusion, Knudsen flow, and Poiseuille flow (Ryu et al., 2016). Mathematical modeling can describe C, depending on the dominating mass transfer mechanism. Several researchers (Lawson and Lloyd, 1996, Ryu et al., 2016) have utilized DCMD modeling a Knudsen-molecular diffusion transition model. Another approach to consider is devising semi-empirical equations using experimentally determined mass transfer coefficients (Winter et al., 2011).

2.9.2. Removing competitive ions from seawater and brine before lithium recovery.

Controlled chemical precipitation, i.e., reactive crystallization, is a widely used and proven technology that can remove metals and other inorganic compounds from wastewater or industrial streams. The removal of calcium as an insoluble carbonate is a well-known water softening and industrial method, in which calcium ions are exchanged for ions with much higher solubility, for example, sodium:

$CaCl_{2\,(aq)} + Na_2CO_3 >> CaCO_{3\,(s)} + 2NaCl_{\,(aq)}$

The produced calcium carbonate can potentially be sold and used extensively for commercial purposes, such as industrially in filler material for paper, plastics, and rubber, as a neutralizing agent in the PAL process (Söhnel and Mullin, 1982). However, Reaction 3 adds sodium to the solutions that will be recycled, which may not be acceptable from the perspective of process chemistry.

Another potential hydrometallurgical implementation of a well-known analytical chemical reaction used in measuring dissolved calcium is the precipitate as insoluble calcium oxalate monohydrate. Here the following equation is used for this purpose:

$CaCl_{2\,(aq)} + H_2C_2O_{4\,(aq)} >> CaC_2O_{4\,(s)} + 2\,HCl_{\,(aq)}$

Chi and Xu (1999) undertook speciation calculations of oxalic acid as a function of pH, and they reported hydrogen oxalate ($HC_2O_4^-$) as the main species at lower pH. It may serve as a ligand making possible the formation of soluble complexes with Ca^{2+} and Mg^{2+}. The fully dissociated oxalate anion ($C_2O_4^{2-}$), responsible for constructing insoluble calcium oxalate, only predominates at pH N7 (50% abundance at pH of 4.5). Due to the PAL practice having process constraints, pH levels higher than 7 are not an option; consequently, to maintain a high enough level of oxalate ions in the solution, an excess of oxalic acid is beyond the stoichiometric requirement will be required. Unlike oxalic acid, the dissociation of oxalate salts is not pH-dependent and thereby creates conditions favoring maximum oxalate species in solution. Using sodium oxalate ($Na_2C_2O_4$) instead of oxalic acid for more efficient precipitation thus becomes an exciting alternative. Calcium can be a beneficial component, and it can exist as quicklime (calcium oxide), limestone (calcium carbonate), and slaked lime (calcium hydroxide)(Lalasari et al., 2019).

Magnesium can be removed from seawater and brine water using sodium hydroxide based on the theory.

$MgCl_2 + 2\ NaOH >> Mg(OH)_2 + 2\ NaCl.$

Maximum Mg^{2+} removal productivities were achieved using sodium hydroxide at pH 12. Magnesium is used as a metal for a variety of construction industry purposes.

2.9.3. Embedding metal-organic framework with manganese oxide ion-exchange adsorption

Factors that can significantly enhance the performance of adsorbents towards ion selectivity include fine-tuning its selective mechanism and increasing its surface ratio. Metal-organic frameworks (MOFs), a new-age material, are highly promising in this regard, as they offer an extraordinarily high surface area with the flexibility to manipulate its pore geometry, size, and functionality for attaining high selectivity of a specific ion.

MOFs are crystalline structures made by the strong bonding of metal clusters with organic functional groups/ligands (Furukawa et al., 2013, Dias and Petit, 2015). The unique features of MOFs in terms of their high surface area and flexibility to modify the size, pore geometry, and functionality has led to the discovery of many types of MOFs that have been applied in various endeavors such as gas separation catalytic processes, sensors, and drug delivery (Furukawa et

al., 2013, Dias and Petit, 2015). Chemical modification resulting in water-stable MOFs is at the forefront of applying MOFs for water remediation. Specifically, the synthesis of water-stable MOFs with characteristics such as ion exchange trapping, surface charge binding, and protonation of functional groups has made possible its application for valuable metal recovery and adsorption of heavy metals even in trace concentrations. For instance, As and Cd in trace levels in wastewater were adsorbed using Zr-based MOF-808 (Efome et al., 2018, Li et al., 2015). Likewise, a modified Fe-BTC MOF exhibited high selectivity for Au in trace concentrations from a mixed water solution (Sun et al., 2018).

CHAPTER 3

MATERIAL AND METHODS

3. Methodology

3.1 Materials

3.1.1. Chemicals and Solutions

A model Li^+ solution (5.0 mg/L) and natural seawater were used to evaluate the performance of HMO for selective Li uptake. Seawater used in this study was collected from Sydney Institute of Marine Science, Chowder Bay, Australia. The characteristics of the seawater are presented in Table 3. The Li^+ concentration in the model Li^+ solution (5.0 mg/L) was substantially higher compared to that present in seawater (0.2 mg/L). Higher Li^+ concentration was used to ensure consistent analytic interpretation at equilibrium condition, as well as to clearly demonstrate the mechanism trend of HMO towards selective Li^+ uptake. Further, model solutions of Li^+ with Na^+, Mg^{2+}, and Ca^{2+} were used to evaluate the effect of ions present in diverse constituents in seawater.

Stock chemical (Na^+, Mg^{2+}, Ca^{2+}, and Li^+) solutions were obtained by mixing respective chemical chloride salts (NaCl, $MgCl_2$, $CaCl_2$, and LiCl) in deionized water (DI water). Analytical grade chemical salts obtained from Sigma-Aldrich (US) were used for preparing the chemical solutions.

Seawater was also used as a feed solution for MD concentrate treatment. Further, pre-treated seawater containing minimal divalent of Ca^{2+} and Mg^{2+} was used to evaluate the influence of inorganic ions in seawater on DCMD. Divalent reduced seawater was achieved by chemical pre-treatment using oxalic acid as an oxidating agent and NaOH as an alkalizing chemical agent.

Table 3: Key characteristics of seawater

Parameter	Value
Total dissolved solids (TDS)	35000 mg/L
Turbidity	0.3±0.2 NTU
Dissolved organic carbon (DOC)	1.6 ± 0.7 mg/L
Ph	8.0±0.3
Ca^{2+}	416.81 ±0.40 mg/L
Mg^{2+}	1414.80±1.60 mg/L
Na^+	11393.51 ±3.22 mg/L
K^+	420.31 ±2.1 mg/L

Parameter	Value
Sr^{2+}	7.835 ± 0.71mg/L
Li^{+}	0.18±0.02 mg/L
Rb^{+}	0.18±0.02 mg/L

3.1.2. Membrane

The DCMD experiments was carried out using polytetrafluoroethylene (PTFE) commercial hydrophobic Membrane (General Electric, US). The membrane characteristics (thickness, porosity, pore size and contact angle) was 178–180 µm, 70–80%, 0.20–0.22 µm and 138.6 ± 2.7° respectively and total effective area of 40 cm^2 was used for all DCMD experiments.

3.1.3. Manganese oxide ion sieve

Lithium manganese oxide (LMO) was used for Li extraction evaluation. The ion sieve particle was synthesized using solution of LiOH solution and Mn_2O_3 powder. Analytical grade chemical salts obtained from Sigma-Aldrich (US) were used without further purification.

3.1.3. HMO@ZIF-8

Stock solutions of 2-methylimidazole (Hmim), zinc nitrate and sodium hydroxide were obtained by mixing respective chemicals (HMIM, $ZnNO_3$, NaOH) in deionized water (DI water). Analytical grade chemical salts obtained from Sigma-Aldrich (US) were used for preparing the chemical solutions. A model Li^{+} solution (5.0 mg/L) was used to evaluate the performance of HMO@ZIF-8 for selective Li^{+} uptake. Further, seawater and model solutions of $^{+}$ with Na^{+}, Mg^{2+}, and Ca^{2+} were used to evaluate the effect of ions present in mixed solution.

3.2. Methods

3.2.1. Manganese oxide ion sieve synthesis

Manganese oxide ion sieve synthesis A hydrothermal process was used to synthesis lithium manganese oxide (LMO), based on the procedure of Chitrakar et al. (Chitrakar et al., 2001). In brief, the synthesis was carried out by mixing 10 g of Mn_2O_3 with LiOH (4.0 M, 200 mL) solution. The solution was stirred homogenously for 6 h in room temperature (24.0 ± 0.5 °C). Next, the solution was placed in a Teflon-lined stainless autoclave hydrothermal reactor and heated at 120 °C for 24 h. Thereafter, the precipitate was centrifuged (3000 rpm) for 10 mins and filtered. The filtered residue was rinsed several times with DI water and oven dried at 50 °C for 12 h. Next, the dried product was grounded with mortar and pestle and sieved (using Standard Testing Woven Wire Mesh Sieves) to obtained homogenous powder. The powder

form LMO (2.0 g) was immersed in HCL (0.5 M, 2.0 L) and stirred (120 rpm) for 24 h at room temperature. This step is to facilitate LMO delithiation (Li^+ to H^+ exchange), producing acid manganese oxide (HMO). The final HMO was washed repetitively with DI water, vacuum filtered and thereafter, oven dried at 40 °C for 12 h. The synthesized HMO was kept in an airtight container.

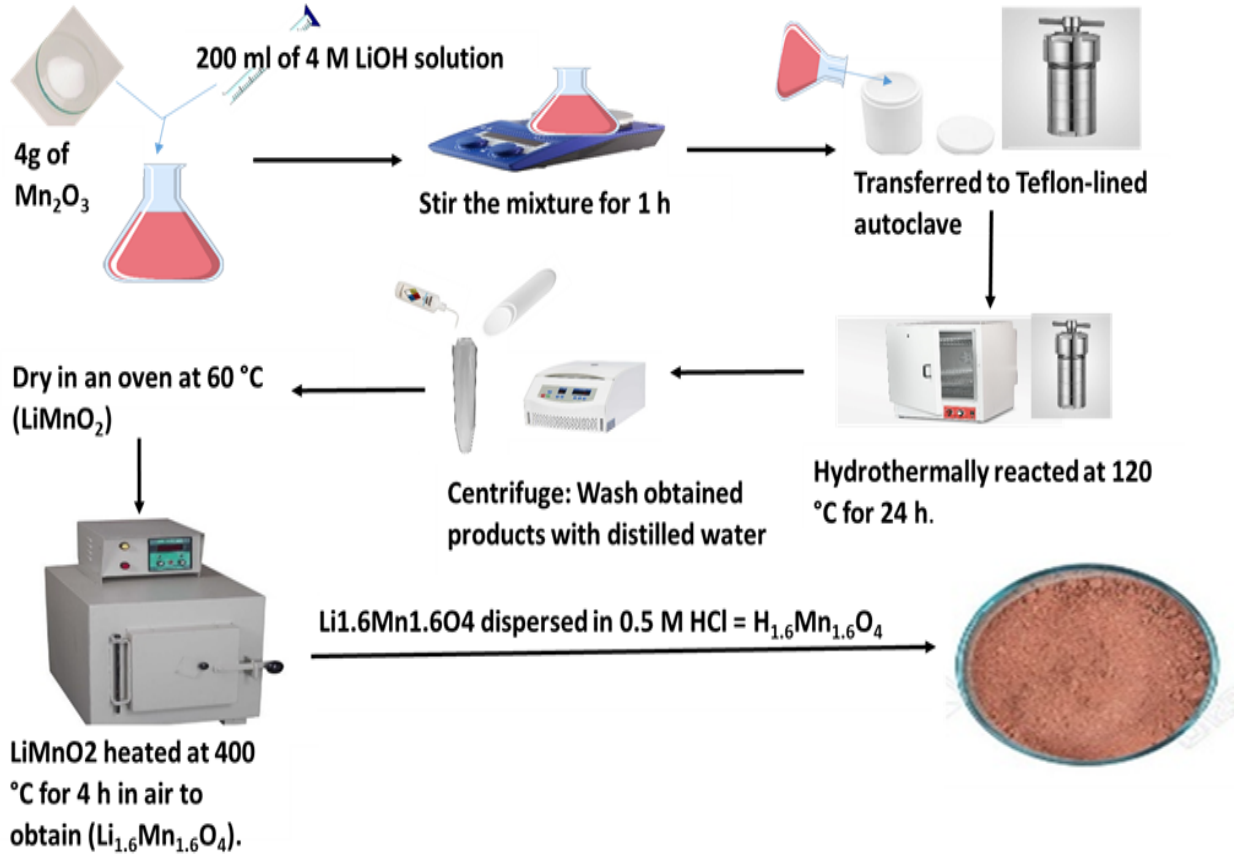

Figure 3: Schematic illustration of the H1.6Mn 1.6O4 adsorbent preparation method

3.2.2. Seawater chemical pre-treatment

Seawater chemical pre-treatment was carried out using two different methods, oxalic acid and caustic soda ash method. For the oxalic acid method, oxalic acid at different doses were added to 100 mL seawater in beakers. The beakers were kept in suspension (120 rpm speed) for 24 h at room temperature (24.0 ± 0.5°C). Thereafter, Mg^{2+} precipitation was carried out by adding NaOH at varied pH (pH 9–12). The beakers were placed in a shaker (120 rpm speed) for 48 h. At the end of each step, seawater samples were filtered using a vacuum filter with glass microfiber filter (Filtech, Australia, 1.1 µm average pore size) to remove and separate the precipitated salts. For the caustic soda ash beaker method, different doses of Na_2CO_3 were added to seawater at varied pH from 9 to 12 using NaOH. The beakers were kept suspended

for 24 h. Dissolved ion contents of the initial and final filtered seawater samples were measured to determine the Ca^{2+} and Mg^{2+} removal rate.

3.2.3. Direct contact membrane distillation (DCMD)

A lab scale DCMD was used to treat and concentrate seawater and pre-treated seawater (Fig. 2). The lab scale DCMD was operated with a PTFE membrane module with a length, width, and channel depth of 8.10 cm × 5.10 cm × 0.23 cm respectively (total active membrane area of 40 cm^2). DCMD was operated with a feed and permeate temperature of 55 °C and 25 °C as discussed in our earlier work (Castillo et al., 2019, Naidu et al., 2017). A 1.8 L volume of initial feed and permeate solution was used and the solutions were recirculated in counter-current mode at a flow rate of 0.5 L/min (translating to a flow velocity of 0.08 m/s). Seawater was treated and concentrated with DCMD by up to 85% water recovery (corresponding to an initial feed volume decrease of 1.80 L to around 0.36 L) or up to near- zero decline flux condition. The distillate/ permeate production was presented as permeate flux (L m−2 h−1 (LMH)) which was computed by permeate volume (L) increment ratio over membrane area (m2) and operation duration (h). Automated balance was used for capturing the mass changes of the permeate solution (DI water as initial permeate solution). In this study, the permeate flux was categorised as a function of the water recovery rate along with volume concentration factor (VCF).

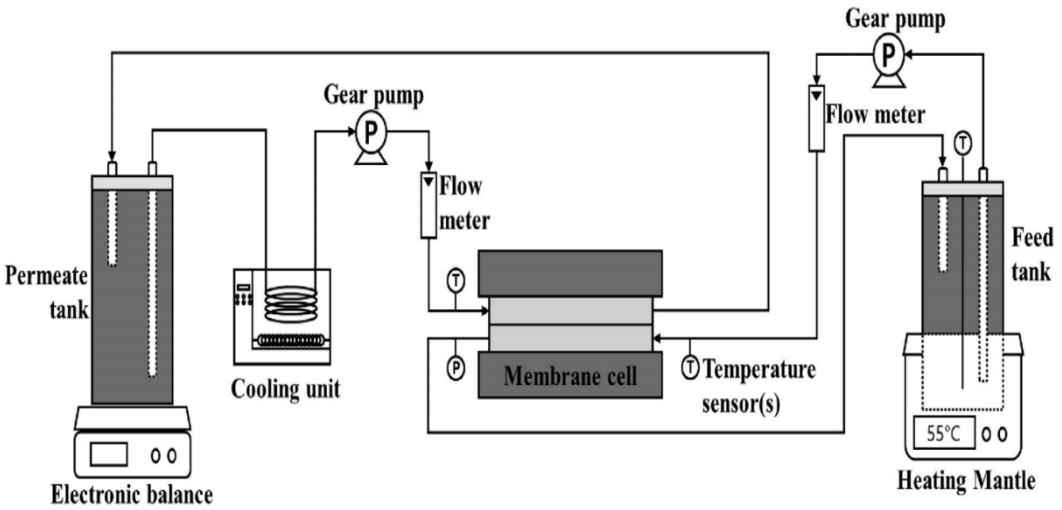

Figure 4: Experimental setup of DCMD

3.2.4. Adsorbent experiments

Adsorbent experiments were carried in batch beaker containing pre-determined amount of HMO with 100 mL of solutions and kept suspended with mixing at 120 rpm. The initial and final ion concentrations was measured with inductively coupled plasma mass spectrometry (ICP-MS) (Agilent 4100). Test were replicated and the standard average were reported. The difference between replicates were less than ± 4%.

3.2.4.1. Influence of pH

Influence of pH on Li^+ uptake at Equilibrium was examined at base and acid settings. HMO, at a dose of 0.05 g/L was placed in beakers with 5.0 ± 0.5 mg Li^+/L solution in the pH ranges of 2 to 12. The beakers were stirred (120 rpm) for 24 h in room temperature. Initial pH values were changed with a few drops of concentrated acid (HCl) and base (NaOH) solution. Measurement of the solution initial pH (pH in) and final/equilibrium pH (pH eq) was recorded.

3.2.4.2. Equilibrium and kinetic studies.

Equilibrium evaluation was conducted in a batch mode using model Li^+ solution (100 mL) in a beaker at varied HMO doses (0.02 g/L−0.20 g/L). The solution pH was maintained at an optimum value per pH evaluation (see Section 2.2.4.1). To attain Equilibrium, the beakers were stirred (120 rpm) using a flat shaker at room temperatures (24 ± 1 °C) for 24 h. For the kinetic study, a fixed sorbent dose (selected based on equilibrium results) was used. Sample collection was carried out at 20 mins time intervals by up to 1440 mins. Equilibrium and kinetics a model used for this study is described below.

3.2.4.2.1. Equilibrium study

The adsorptive capacity of HMO at Equilibrium, Q_e (mg/g), is represented as:

$$Q_e = V(C_0 - C_e)/M \quad (1)$$

where C_0 and Ce (mg/L) are initial and equilibrium Li^+ concentration (mg/L); V is solution volume (L), and M is HMO mass (g) (Naidu et al., 2016).

Two typical isotherm models (Langmuir and Freundlich) were used to represent the equilibrium data. The model equations were represented using Eq (2) and (3) as below:

Langmuir isotherm: $Q_e = Q_m b C_e/(1 + bC_e)$ (2)

Freundlich isotherm: $Q_e = K_F {C_e}^{1/n}$ (3)

where, Q_m and b are the maximum sorption capacity (mg/g) and Langmuir constant (L/mg) representing binding site affinity. Freundlich constant is related to sorption/uptake tendency, K_F (g^{1-n} $L^n g^{-1}$) and 1/dimension less parameter (1/n) was related to the heterogeneity of the adsorbent surface.

3.2.4.2.2. Kinetics

The kinetic data was represented using pseudo first and second order models, as described by Eq. (4) and (5).

$$\text{Pseudo first order: } Q_t = Q_e(1 - e^{-k_1 t}) \quad (4)$$

$$\text{Pseudo second order: } t/Q_t = 1/k_2 Q_e{}^2 + t/Q_e \quad (5)$$

The parameters, Q_t and Q_e are the adsorption capacity (mg/g), k_1 and k_2 express the adsorption rate (h^{-1}) and t is the time (h) duration of the process.

3.2.5. Desorption and regeneration

Desorption and regeneration. The reusability of HMO was tested with multiple adsorption and desorption cycles in batch mode. Adsorption was carried out using HMO at a dose of 0.1 g/L with model Li^+ solution. The used HMO was filtered from the working solution and dried at room temperature. Desorption was carried out using HCl based on the Li^+/H^+ exchange mechanism [18,39]. Firstly, different HCl concentration was tested. Specifically, Li-saturated HMO was placed in a beaker with 30 mL of HCl at different concentrations (0.05 M to 1.0 HCl) and kept suspended (120 rpm) for 24 h. Subsequently, upon identifying the optimum HCl concentration, multiple cycle of adsorption and desorption was carried out. The concentration of initial and final $Li^+$and dissolved Mn^{4+} were measured using ICP-MS.

3.2.6. Synthesis and grafting of Zeolitic imidazolate framework ZIF-8 and HMO@ZIF-8

3.2.6.1. Zeolitic imidazolate framework ZIF-8

Typically, ZIF-8 to produce by procedure of Xue Min et al. (Xue Min et al., 2017). In brief, the synthesis was carried out by 2-methylimidazole (3.0 M, 16 mL) solution was mixed Next, with zinc nitrate (0.84M, 1.6mL) and sodium hydroxide (0.1M, 0.1 mL) solutions homogenously at 1600rpm for 3min. Then the solution was placed in a thermo shaker to stirred (120rpm) and heated at 40 °C for 30 minutes. Thereafter, the solution was centrifuged (9300 rpm) for 10 mins and filtered. The filtered residue was washed three times with ethanal using centrifuged (5000 rpm for 4 mins) and oven dried at 50 °C for overnight. Next, the dried

product was grounded with mortar and pestle and sieved (using Standard Testing Woven Wire Mesh Sieves) to obtained homogenous powder.

3.2.6.2. Grafting ZIF-8 with H-form manganese oxide (HMO), HMO@ZIF-8

H form manganese oxide (HMO) grafting with ZIF-8 to produce HMO@ZIF-8 is based on the procedure of Xue Min et al. (Xue Min et al., 2017). In brief, the synthesis was carried out by mixing 246 mg of H form manganese oxide with 2-methylimidazole (3.0 M, 16 mL) solution. The solution was mixed homogenously at 1600rpm for 3min. Next, zinc nitrate (0.84M, 1.6mL) and sodium hydroxide (0.1M, 0.1 mL) solutions were added into the mixed solution. Then the solution was mixed homogeneously at 1600rpm for 3 minutes. then placed in a thermo shaker to stirred (120rpm) and heated at 40 °C for 30 minutes. Thereafter, the solution was centrifuged (9300 rpm) for 10 mins and filtered. The filtered residue was washed three times with ethanal using centrifuged (5000 rpm for 4 mins) and oven dried at 50 °C for overnight. Next, the dried product was grounded with mortar and pestle and sieved (using Standard Testing Woven Wire Mesh Sieves) to obtained homogenous powder.

3.3. Analysis

3.3.1. Solution concentration and characterization.

The ion concentrations of seawater and model solutions were determined by ICP-MS. The solution pH and total dissolved solids (TDS) were measured using a portable meter (model HQ40d HACH, US). The DOC content was measured using dual peak liquid chromatography with organic carbon detection (LC-OCD).

3.3.2. Membrane characterization

The new (virgin) and used Membrane upon DCMD experiments will be characterized in terms of surface hydrophobicity (contact angle) and morphology. Contact angle measurements will be carried out using a water droplet goniometer (Theta Lite) on the virgin and used Membrane (upon drying). Membrane surface morphology and element contents (virgin and used membranes) will be examined using scanning electron microscope (SEM) integrated with energy-dispersive spectroscopy (EDS) as described in a previous study (Naidu et al., 2017)

3.3.3. Adsorbent characterization.

Manganese oxide ion sieve and membrane characterization the new (virgin) and used DCMD membranes were characterized in terms of hydrophobicity (water contact angle) and morphology of its surfaces (upon drying). Membrane surface hydrophobicity was measured with water contact angle using goniometer (Theta Lite). Meanwhile, the morphology and ion

contents of the Membrane and HMO (unused and upon Li^+ uptake) were examined by scanning electron microscope (SEM) operated at 15 kV (Zeiss Supra 55VP Field Emission) combined with energy-dispersive spectroscopy (EDS) as described by our previous studies (Castillo et al., 2019, Naidu et al., 2017). Changes on crystal structure of HMO was determined by X-ray powder diffraction (XRD) (Siemens D5000 diffractometer). XRD was operated with CuK alpha-radiation and sample stage that is rotating. Powder-form HMO (unused and upon Li^+ uptake) were scanned at room temperature in the 2^{Θ} angular range of 20–110°. HMO surface charges were detected using zeta sizer analyser (Nano ZS Zen3600, Malvern, UK). HMO (0.05 g/L) was suspended and agitated (120 rpm) in beakers containing 100 mL of LiCl (5.0 mg/L) in pH range of 3–11 for 24 h.

CHAPTER 4

RESULTS AND DISCUSSION

4. Results and discussion

4.1. Seawater chemical pre-treatment

The addition of oxalic acid enabled to minimize Ca^{2+} content in seawater by forming insoluble calcium oxide precipitation (Eq. (1)) (Moldoveanu and Papangelakis, 2015) A by-product of oxalic acid addition to seawater is HCl formation that contributed towards reducing the pH of seawater from 8.0 ± 0.5 to 3.0 ± 0.5.

$$CaCl_{2\ (aq)} + H_2C_2O_{4\ (aq)} = CaC_2O_4\ (s) + 2\ HCl_{\ (aq)} \quad (1)$$

Higher Ca^{2+} removal from seawater was achieved by increasing oxalic acid dosage from 0.1 g/L to 3.0 g/L (Fig. S1). From a dose of 2.5 g/L oxalic acid onwards, 92–95% removal of Ca^{2+} was achieved, indicating this to be the optimal dose. As such, 2.5 g/L dose of oxalic acid was used for all further Ca^{2+} removal experiments (Table 4).

Table 4: Key parameters of original and pre-treated seawater.

Parameters	**Concentration (mg/L)**							
	pH	DOC	Na^+	Mg^{2+}	Ca^{2+}	K^+	Sr^{2+}	Li^+
Original seawater	8	1.6-2.0	13642.38	1294.56	377.11	389.81	7.30	0.17
Pre-treated seawater								
Oxalic acid and GAC	3	4.0-5.0	10473.44	1293.10	6.72	390.20	3.00	0.17
Na_2CO_3 and NaOH	10	1.6-2.0	14083.23	901.64	22.63	341.37	3.55	0.17

At the same time, conventional caustic soda ash approach (addition of Na_2CO_3, combined with NaOH) was also used for Ca^{2+} removal from seawater (Sanmartino et al., 2017). In this approach, Ca^{2+} was removed as $CaCO_3$. NaOH was used to neutralize carbonic acid and to increase seawater pH, as Ca^{2+} precipitation is enhanced at higher pH (pH 9 and above). At Na_2CO_3 dose of 3.0 g/L onwards, it was possible to achieve over 90% Ca^{2+} removal from seawater (Fig. S1, Table 3). However, the disadvantage of the caustic soda ash approach is that it resulted in an increase in Na content in alkaline condition (hydroxide residue). This apart, Ca^{2+} removal occurred simultaneously with 26–30% Mg^{2+} removal. In this scenario, to attain pure Ca^{2+}, further purification steps will be required to separate Mg^{2+} from Ca^{2+}. The separation of Mg^{2+} from Ca^{2+} can be challenging given both are divalent ions with similar chemical characteristics.

Comparatively, the approach of using oxalic acid was beneficial for achieving selective Ca^{2+} removal from seawater without simultaneous Mg removal. Further, the oxalic acid reduced Na concentration by about 23%. Contrarily, the caustic soda ash method increased the Na content, invariably increasing the overall ion concentration in seawater. Nevertheless, the addition of oxalic acid significantly increased the organic contents in seawater (DOC of 2.0 ± 0.4 mg/L to 32.2 ± 0.3 mg/L). A simple granular activated carbon adsorption was used to remove the organic content. At a dose of 6.0 g/L granular activated carbon, the organic content of oxalic acid treated seawater was reduced to 4.5 ± 0.5 mg/L (Fig. S2). Given the toxicity of oxalic acid, granular activated carbon pre-treatment could be used to remove the remaining/residue oxalic acid in concentrated seawater prior to its disposal if required. Comparatively, with the caustic soda ash approach, it is a challenge to reduce the salinity (dissolved sodium/salt contents) of concentrated seawater prior to disposal.

4.2. Performance of DCMD with seawater and pre-treated seawater

4.2.1. Permeate flux and characteristics.

DCMD performance with seawater and pre-treated seawater as feed solutions achieved similar initial permeate fluxes of 25.5 ± 0.8 L/m2 h (LMH) (Fig. 2). The similar initial permeates fluxes suggest that the initial variation of ion concentration in the feed solution minimally influenced the driving force, given that the same feed temperature difference was used for all experiments. Likewise, in a recent study, Kim et al. reported similar initial permeate fluxes with seawater as well as Ca^{2+} and Mg^{2+} reduced seawater. It is well established that vapour pressure (driving forces) in MD is minimally influenced by small variation in salt content (water activity) of the feed solution while its impact is apparent in highly supersaturated brines (Guan et al., 2018). This is because water activity only changes minimally (from 1.0 to 0.95) even when the molarity of NaCl is significantly varied (from 0.01 M to 2.00 M). For all conditions, the permeate characteristics was of high quality throughout the experimental duration. Specifically, the final permeates solutions showed conductivity (less than20 µS/cm) levels similar/lower to that of the initial permeate solutions and concentration of the major ions showed 98 ± 2% ion rejection (Table SI). In terms of permeate flux trend over volume concentration factor (VCF), DCMD operated with seawater and caustic soda ash pre-treated seawater exhibited rapid decline of permeate fluxes (86–90%) by VCF 3.0 onwards. Typically, seawater, in its original condition contain Ca^{2+} in the range of 350–400 mg/L. It is highly challenging for MD to treat original seawater due to the inevitable development of Ca^{2+} based scaling in thermal condition, namely, $CaSO_4$. As seawater is concentrated over time, $CaSO_4$

scalant deposition onto the Membrane resulted in permeate flux decline. This phenomenon has been well established by several previous studies (Mericq et al., 2010, Naidu et al., 2015, Choi et al., 2017). It is likely that $CaSO_4$ deposition only occurred on the surface of the Membrane and did not go through the pores. Therefore, permeate with high quality was still maintained throughout the experimental duration.

Given the dominant role of Ca scalant in reducing MD performance, minimizing Ca content in seawater, such as that of caustic soda ash softening, is therefore, expected to mitigate scaling issue and enhance MD performance towards concentrating seawater. In line with this, the results of this study show that seawater treated with caustic soda ash (containing reduced Ca^{2+}) enabled to achieve better performance to that of original seawater. Nevertheless, by VCF 4.0 (65–68%), significant permeate flux decline occurred. This could be attributed to several factors. Firstly, caustic soda ash approach increased the Na content through the addition of sodium (hydroxide and carbonate), invariably increasing the overall salinity and ion content of the feed solution. In MD, high salinity of the feed solution reduces vapour pressure, which in turn, reduces the driving force, resulting in permeate flux decline (Mericq et al., 2010, Winter et al., 2011, Eykens et al., 2016, Guan et al., 2018). Secondly, caustic soda ash approach occurs in alkaline condition with the addition of both hydroxide and carbonate. In thermal MD process, the residues of hydroxide and carbonate in alkaline condition, increases susceptibility towards inorganic scalant formation (Qu et al., 2009). The formation of scalants that deposits onto the Membrane, compromises the capacity of MD to further concentrate seawater.

On the other hand, DCMD effectively concentrated seawater treated with oxalic acid by up to VCF 7.8 (88–91% water recovery) with a gradual permeate flux decline from 25.5 ± 0.8 L/m2 h to 8.5 ± 1.4 L/ m2 h (approximately 72% flux decline) (Fig. 5). The capacity of DCMD to concentrate oxalic acid treated seawater by up to VCF 7.0 could be attributed to the reduced initial ions in seawater, given that apart from 95% Ca^{2+} removal, oxalic acid also simultaneously removed 23% of Na (Table 3). This apart, the final ion mass balance of the DCMD concentrated seawater indicated reduction/losses of major ions (Table 4). Specifically, Na mass losses (26%) occurred during the DCMD treatment. As the concentration of ions in oxalic acid treated seawater did not increase proportionally with volume concentration factor (VCF) during DCMD, it is likely that the negative effect of vapor pressure reduction with high salinity and concentration effect was minimized. This may have likely prevented the early and rapid flux decline trend that occurred with seawater and caustic soda ash treated seawater. Further, compared to the alkaline condition of caustic soda ash seawater (pH 9.0 ± 0.5),

addition of oxalic acid resulted in an acidic condition (pH 3.0 ± 0.5). The acidic condition was beneficial to delay induction of ion precipitation (Gryta, 2010). Specifically, the high Na mass losses indicated the occurrence of Na precipitation as it was concentrated in DCMD. However, it is likely that the acidic condition of the feed solution delayed ion induction and therefore, Na precipitation occurred only at the later duration of the DCMD operation. In line with this, gradual permeate flux decline occurred towards the final stages of the operation. Further, although precipitation of major ions occurred as seawater was concentrated/saturated, similar Li mass was maintained (Table 5).

Table 5: Ion concentration and mass of pre-treated seawater with oxalic acid with DCMD.

Oxalic acid treated seawater	**Ion content**	**Na^+**	**Mg^{2+}**	**Ca^{2+}**	**K^+**	**Sr^{2+}**	**Li^+**
Initial (1.80L)	Concentration (mg/L)	10473.44 ± 1.06	1293.18 ± 0.63	6.72 ± 0.08	390.20 ± 0.72	3.00 ± 0.02	0.17 ± 0.01
	Mass (mg)	18852.19 ± 0.78	2327.72 ± 0.33	12.10 ± 0.07	702.36 ± 0.46	5.40 ± 0.01	0.31 ± 0.02
Final (0.25L)	Concentration (mg/L)	55339.73 ± 1.21	8498.63 ± 0.77	47.38 ± 0.11	2484.14 ± 0.62	15.90 ± 0.06	1.22 ± 0.02
	Mass (mg)	13890.27 ± 0.89	2133.16 ± 0.54	11.89 ± 0.03	623.52 ± 0.45	3.99 ± 0.03	0.31 ± 0.01
Mass Loss (%)		26.32	8.35	1.68	11.22	26.09	-

The insignificant losses of Li^+ could be due to its high solubility and low concentration in seawater. Overall, the results of this study highlight the suitability of oxalic acid as a seawater chemical pre-treatment to minimize Ca scaling and effectively concentrate seawater in DCMD with insignificant losses of L^+i. In effect, this condition enabled to increase Li^+ concentration in seawater by 7 times from 0.17 mg/L to 1.22 mg/L, while achieving 86% water recovery (producing high quality fresh water).

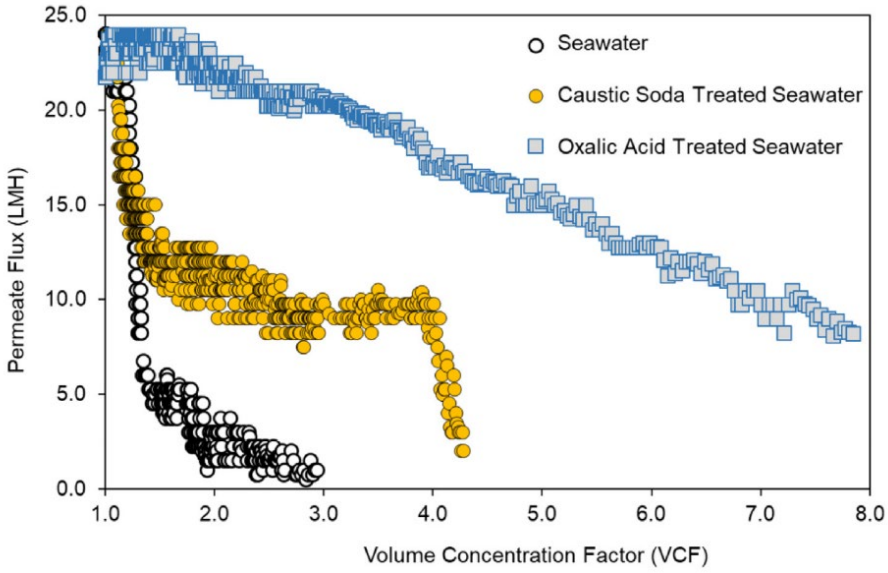

Figure 4: DCMD permeate flux trend as a function of VCF with seawater and pre-treated seawater using caustic soda ash and oxalic acid (VCF = volume ratio of initial to final feed solution, represents the degree of volume reduction of the feed solution).

4.2.2. Membrane analysis.

Detailed membrane analysis (SEM-EDX) and contact angle evaluation was carried out to establish the effectiveness of oxalic acid pre-treated seawater. Used Membrane with seawater contained high Ca^{2+} (Fig. 3a). Further the hydrophobicity of the used Membrane with seawater (water contact angle of 92.2 ± 1.4°) was reduced by 40% compared to the virgin Membrane (water contact angle of 138.6 ± 2.7°). This verified the development of $CaSO_4$ scaling that compromised the performance of DCMD with untreated seawater. Both used membranes with pre-treated seawater of caustic soda ash and oxalic acid did not contain Ca^{2+}, indicating the effectiveness of both treatment approaches to minimise Ca^{2+} content in seawater. However, significant presence of Mg^{2+} and Na^{+} was detected on used Membrane with caustic soda ash treated seawater (Fig. 6b). The high Mg^{2+} formation was most probably due to the addition of NaOH at pH above 9 that resulted in the formation of $Mg(OH)_2$ that adhered strongly onto the membranes. Further, higher Na concentration with the addition of Na_2CO_3 resulted in clear formation of Na on the Membrane. The water contact angle of the used Membrane with caustic soda ash treated seawater was 71.6 ± 1.4°. Comparatively, the used DCMD membrane with oxalic acid treated Membrane showed the presence of only high Na. This was in line with the observation discussed in Section 3.2.1 on the flux decline at VCF 7.8 and the high Na mass losses with oxalic acid treated seawater (Table 4). It is important to note that visible colloids were formed with oxalic acid treated seawater and this is likely attributed to the high organic

content. Further the water contact angle was also reduced to 87.7 ± 0.7°. However, upon washing with citric acid, the colloids on the Membrane was easily removed and the hydrophobicity (water contact angle of 132.4 ± 3.8°) was comparatively similar to that of the virgin Membrane (Fig. 6).

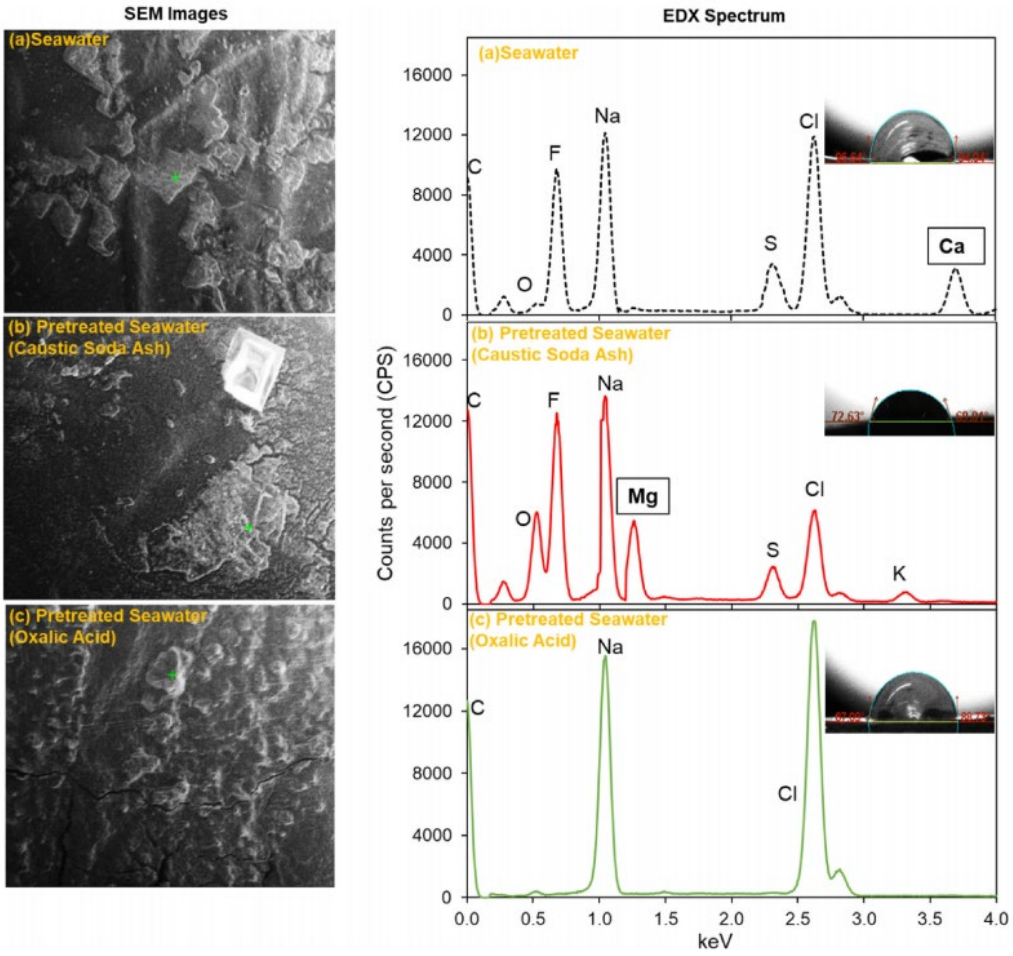

Figure 5: SEM EDX of used DCMD membranes with seawater (VCF 3.0), caustic soda ash treated seawater (VCF 4.2) and oxalic acid treated seawater (VCF 7.8).

4.3. Li^+ extraction by HMO

4.3.1. HMO characteristics

The XRD pattern of acid treated manganese oxide (HMO) and used (Li^+ extracted) HMO is presented in Fig. 7a. The XRD diffraction peaks show a similar trend, with relative peak shift and marginal changes to the intensities. The results were consistent with previous studies (Park et al., 2014, Shi et al., 2011, Tian et al., 2010, Xiao et al., 2015). The slight peak shift towards higher diffraction angle in the used HMO compared to original/unused HMO could be attributed to delithiation of Li^+ with H^+. For instance, Xiao et al. (Xiao et al., 2015) reported on the crystal lattice shift (from 8.16 to 8.08 Å) of spinel-type LMO upon treatment with acid and associated this with the contraction of lattice due to Li^+ to H^+ ion exchange. Overall, the similar XRD diffraction pattern/intensity indicated the topotactic Li^+ to H^+ exchange during delithiation and the preservation of the cubic/spinel structure upon delithiation. Similar basic structure of the used and unused/original HMO established that Li^+ extraction and replacement resulted in minimal damage to its structure, which implies the regenerative capacity of HMO. In terms of morphology, the SEM images (Fig. 7b) showed that the HMO composed of dispersed particles with cluster forms of cubic like grains. Similar morphology and particle size distribution (average particle size of HMO and used HMO were 95.4 ± 1.7 nm) were observed between HMO and Li^+ extracted HMO. The results were in line with previous studies (Hong et al., 2013, Park et al., 2014, Ohashi and Tai, 2019).

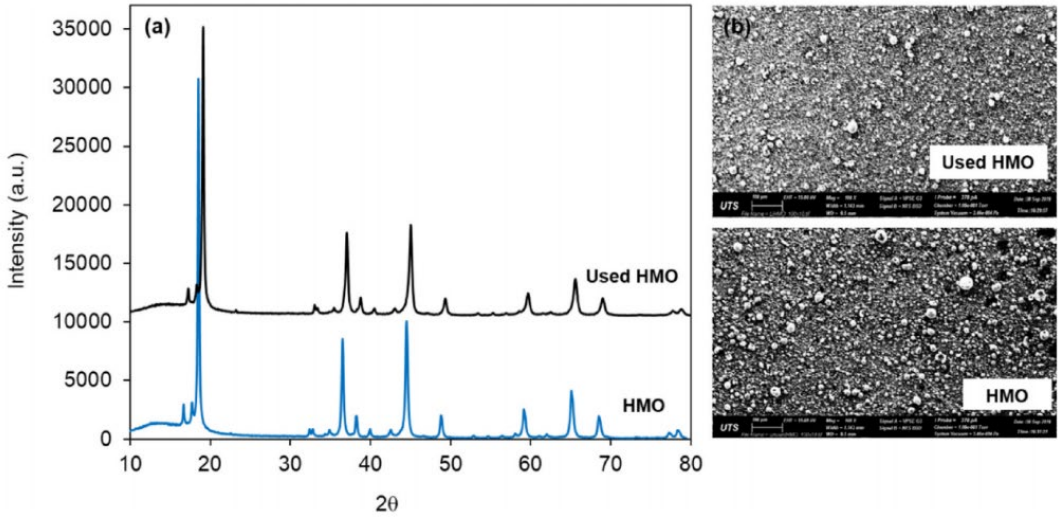

Figure 6: Characteristics of HMO and Li^+ extracted/used HMO (a) X-ray diffraction patterns of (b) SEM morphology images.

4.3.2. Li^+ uptake by HMO

4.3.2.1. Influence of pH and surface zeta charge.

Li^+ uptake increased from less than 2% by up to 98% as the solution pH was increased from 3 to 12 (Fig. 8). This indicated that the solution pH plays a significant role in influencing Li^+ uptake with HMO, as reported in previous studies(Shi et al., 2011, Park et al., 2014, Ryu et al., 2019). To gain a better understanding on the relationship of pH and HMO for Li^+ uptake, the zeta potential (surface charge) of HMO was measured at varied pH ranges. The results showed that the surface charge of HMO became more negative with pH increment. Increased negative surface charge of an adsorbent enhances electrostatic adsorption (outer-sphere ion complexation) of positively charged ions (Naidu et al., 2018). Hence, it is likely that the high negative surface charge of HMO at higher pH (11.5), attracts positively charged Li^+ ion. In turn, higher Li^+ uptake was achieved. At the same time, the presence of high hydroxide ions at pH above 6 provided a favourable deprotonation condition for the removal of H from the ion sieve (Feng et al., 1992, Tian et al., 2010, Shi et al., 2011, Ryu et al., 2019). This condition triggers the exchange of H from the adsorbent with Li^+ from the solution. Correspondingly, it was observed that at pH above 6, the initial pH value showed a reducing pH trend upon Equilibrium, indicating the release of H from the adsorbent sites into the solution. On the other hand, at lower pH, the presence of high H ion in the solution creates an unfavourable condition for deprotonation of H from the adsorbent (Feng et al., 1992, Tian et al., 2010, Shi et al., 2011, Ryu et al., 2019). As a result, minimal vacant sites were made available for the exchange of Li^+ with H. This explains the low Li^+ uptake (below 20%) at pH below 6. It is also worth mentioning that at all pH ranges, only trace concentration of Mn was detected in the solution. These results suggest that Mn desorption from HMO was not influenced by pH change. Moreover, the desorbed concentration of Mn was insignificant compared to the amount of Li^+ adsorbed. As such, Mn in HMO did not play a role in the Li^+ adsorption mechanism. Further, minimal presence of Mn indicates the chemical stability of the adsorbent as observed by previous studies (Shi et al., 2011, Park et al., 2014, Ryu et al., 2019). Overall, the results establish that maximum Li^+ uptake was obtained at pHeq of 11.6–11.8. However, at these pH ranges, precipitation of ions, namely, Ca^{2+} and Mg^{2+} is inevitable in mixed solution such as that in seawater. For this reason, all further experiments were carried out at pHeq of 11.0 ± 0.5 to achieve high Li^+ uptake while ensuring minimal precipitation of divalent ions occur in seawater.

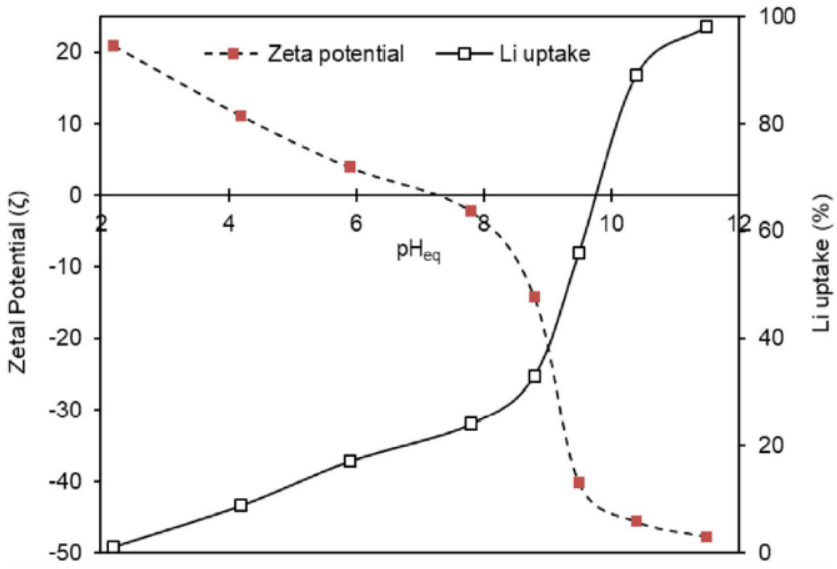

Figure 7: Influence of pH on HMO surface zeta potential and Li^+ uptake.

4.3.2.2. Equilibrium adsorption

4.3.2.2.1. Isotherm.

Isotherm evaluation of HMO for Li^+ uptake was carried out by varying the adsorbent dose (0.05 g/L to 2.00 g/L) at pHeq of 11.0 ± 0.5 for 24 h. The results showed that Li^+ uptake capacity increased synonymously with equilibrium concentration before stabilising at maximum values (Fig. 9a) The experimental data fitted well to both Langmuir and Freundlich isotherm models (R2 = 0.94–0.98). Langmuir model fitting for Li^+ uptake achieved a Q_{max} of 17.8 mg/g. The Langmuir isotherm model assumes saturated single-layer adsorption of the adsorbent surface. The model fitting indicated that Li^+ adsorbed homogeneously onto HMO by forming a monolayer. Similar observations were reported by previous studies for Li^+ uptake by HMO (Park et al., 2014, Shi et al., 2011). For instance, Park et al. reported a Langmuir Q_{max} of 15.1 mg/g for Li^+ uptake with HMO at pH 11 and equilibrium metal concentrations of 7–32 mg/L. Likewise, in a seawater solution spiked with high Li^+ ion (30 mg/L), Hong et al. achieved a Q_{max} of 18.0 mg/g using HMO powder. Higher adsorption capacity can be achieved by increasing the initial solution concentration and adsorption condition such as elevated pH and temperature. For instance, Shi et al. achieved a high Li^+ uptake of 27.2 mg/g with HMO by using a pH above 11 in salt brine containing high Li^+ (300 mg/ L), at elevated temperature of 50 °C. 3.3.2.2.2. Kinetics. The influence of time on Li^+ uptake by HMO is displayed in Fig. 9b. Li^+ uptake increased with time with a trend of rapid Li^+ uptake at the initial stage (0–7 h)

followed by a slow uptake till Equilibrium was attained within 17–24 h. The experimental data was analysed using pseudo first and second order kinetic models (Table 6).

Table 6:Equilibrium batch adsorption isotherm and kinetic model parameters for Li^+ uptake with HMO.

Isotherm models	Langmuir			Freundlich		
	Q_{max} (mg/g)	K_L (L/mg)	R^2	n	K_F (mg/g)	R^2
	17.76	1.13	0.98	2.25	8.34	0.96
Kinetic models	Pseudo-first order (PFO)			Pseudo-second order (PSO)		
	q_e (mg/g)	$K_1 \times 10^{-2}$ (min^{-1})	R^2	q_e (mg/g)	$K_2 \times 10^{-2}$ (min^{-1})	R^2
	5.00	0.11	0.81	8.54	0.41	0.99

The pseudo second order (PSO) model showed a better fitting (R^2 = 0.97–0.98), compared to pseudo first order (PFO) model. Better PSO representation of the experimental data suggest that Li^+ uptake on HMO was predominantly a chemisorption reaction (Naidu et al., 2018), by which, the Li^+ concentration in the solution and the availability of sorption sides on HMO play important roles in influencing Li^+ uptake. The chemisorption reaction description by PSO kinetic model is in line with the H^+-Li^+ exchange mechanism by HMO as established by previous studies (Tian et al., 2010, Park et al., 2014).

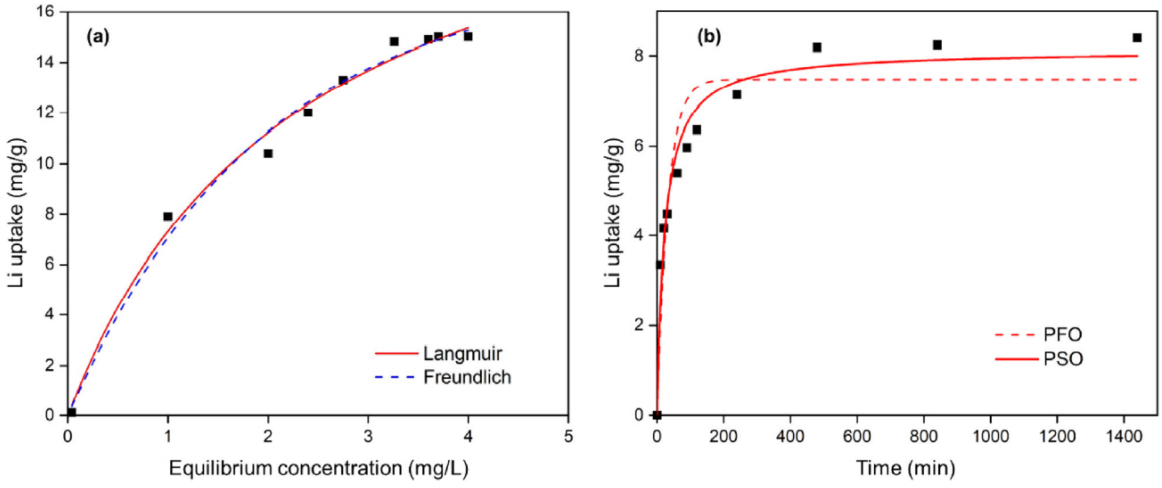

Figure 8: Equilibrium batch adsorption experiments with HMO for (a) Li^+ uptake at different equilibrium concentrations described by Langmuir and Freundlich models (Co = 5 mg Li^+/L; pHeq = 11.0 ± 0.5, time = 24 h); and (b) Li^+ uptake as a function of time described by pseudo first and second order kinetic models (Co = 5 mg Li^+/ L; pHeq = 11.0 ± 0.5, HMO dose = 0.5 g/L).

4.3.3. Influence of ion competition

The influence of ion competition was evaluated by comparing the capacity of HMO for achieving selective Li^+ uptake in a single Li^+ model solution and seawater (original and pre-treated seawater). All experiments were carried out at pHeq of 11.0 ± 0.5 with the same HMO dose. Further, to compare the performance of HMO at the same initial concentration, seawater solutions were spiked with 5 mg Li^+/L as that of the Li^+ model solution. Compared to the model Li^+ solution, Li^+ uptake capacity of HMO reduced by 44–46% in seawater (Fig. 10). Although Li^+ uptake reduced in seawater, HMO was still able to maintain high Li^+ selectivity, with minimal uptake of other major ions (Na^+, K^+, Mg^{2+} and Ca^{2+}) present in high concentrations (400–1700 mg/L) to that of Li^+ (5 mg/L). Specifically, the concentration of Na, and K remained similar before and after HMO adsorption, indicating that the uptake of these ions onto HMO did not occur simultaneously with Li^+ uptake. Meanwhile, only a minimal Ca^{2+} and Mg^{2+} uptake (2–3%) occurred simultaneously with Li^+ uptake. The results of the study was in line with previous studies that evaluated the selective uptake of Li^+ from mixed solution such as seawater, salt lake and geothermal brine. For instance, Park et al. used granular form polymer HMO and reported its capacity to maintain selective uptake of Li^+ with minimal uptake of other major ions from seawater brine spiked with 15 mg/L Li^+. In another study, Xiao et al. reported on the high selective capacity of spinel form HMO towards Li^+ extraction compared to Na, K and Ca^{2+} in Salt Lake brine. Likewise, Wang et al. reported on the capacity of chitosan granulated HMO to selectively extract Li^+ from geothermal brine containing Na^+, K^+ and Ca^{2+} in the background.

Table 7:Concentration of major ions in brine and its ionic characteristics.

Ions	Concentration in seawater (mg/L)	Ionic radius, Å	Electronegativity Scale χ	Hydration enthalpy (kJ/ mol)
Na^+	11,700–13,600	1.02	0.93	−405
Mg^{2+}	1,200–1,300	0.72	1.31	−1922
Ca^{2+}	370–410	1.00	1.00	−1592
K^+	380–390	1.38	0.82	−312
Li^+	0.12–0.18	0.76	0.98	−515

Given that the uptake of major ions were minimal, the significant reduction of Li^+ uptake in seawater compared to single model Li^+ solution could be attributed to non-specific surface

adhesion of these ions on HMO. This may have resulted in surface competition with Li^+, which in turn, reduced Li^+ uptake of HMO. Moreover, it is likely that Na^+, K^+ and Ca^{2+} were unable to pass through the pores of the ion sieve HMO, attributed to the larger ionic radii of these ions compared to Li^+ (Table 6); thus, they only attached to the surface of HMO. Comparatively, the ionic radii of Li (0.76 Å) and Mg (0.72 Å) are closely similar (Table 6). Further, apart from ionic radii, the high electronegativity of Mg^{2+} compared to Li^+ and other ions (Table 6) suggest the strong affinity of Mg^{2+} to adhere onto the negative surface of HMO. Therefore, the presence of Mg^{2+} could be the main ion competitor that reduced Li^+ uptake in seawater with HMO. The strong $^{2+}$ to Li^+ion competition has been highlighted in previous studies (Xiao et al., 2015, Gu et al., 2018, Wang et al., 2020). For instance, Gu et al. reported on the lower Li^+ uptake of H-form titanium oxide with Salt Lake brine compared to model Li^+ solution and associated this with the presence of Mg^{2+} that adhered onto the surface of the adsorbent. To establish the influence of Mg^{2+}, HMO performance for Li^+ uptake was evaluated with two types of pre-treated seawater solution (oxalic acid Ca^{2+} reduced seawater and divalent (Ca^{2+} and Mg^{2+}) reduced seawater).

The results showed that Li^+ uptake by HMO only marginally improved with Ca^{2+} reduced seawater compared to that of the original seawater (Fig. 10). These results indicated that the presence of Ca^{2+} did not play a significant role in influencing Li^+ uptake in seawater. This was in line with the theory discussed above on the inability of Ca^{2+} to pass though the pores of the ion sieve due to its larger ionic size. On the other hand, the divalent (Ca^{2+} and Mg^{2+}) reduced seawater achieved significantly high Li^+ uptake, closely like that of the model Li^+ solution. This result verified that the presence of Mg^{2+} in seawater was the main ion that reduced Li^+ uptake in seawater, compared to the other major ions (Gu et al., 2018, Wang et al., 2018). However, in spite of the high Mg^{2+} to Li^+ concentration ratio, Mg uptake was minimal compared to Li^+ uptake (as observed in original and Ca^{2+} reduced seawater). The high hydration enthalpy of Mg^{2+} (high energy required for Mg^{2+} to attain dehydrated ionic condition) may have played a role in limiting its uptake onto HMO.

Overall, these results indicated seawater with minimal of Mg^{2+}, provides a favourable condition for enhancing Li^+ uptake by HMO in seawater. This necessitates Mg^{2+} removal. In this study, Mg^{2+} removal from seawater was achieved by adding NaOH. The removal of Ca^{2+} with oxalic acid followed by Mg^{2+} removal with NaOH was beneficial in that it enables to produce firstly Ca^{2+} followed by Mg^{2+} from seawater as a by-product. Further, the addition of NaOH for Mg^{2+} removal at pH 11.0 ± 0.5 was a suitable alkaline pH for Li^+ uptake by HMO. Nevertheless, it

is also important to mention that the addition of NaOH for Mg^{2+} removal invariably increased Na content in seawater. As a result, a small amount of Na uptake occurred with Li^+ uptake in divalent reduced seawater.

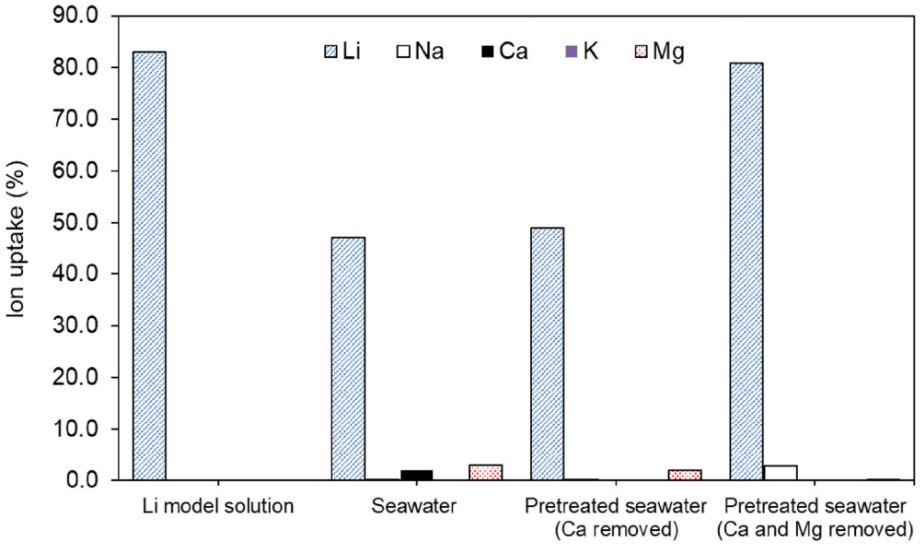

Figure 9: Comparison of ion uptake by HMO in model Li^+ solution, original and pre-treated seawater spiked with Li^+ (Co = 5 mg Li^+/L; pHeq = 11.0 ± 0.5, HMO dose = 0.5 g/L). (Ca^{2+} pre-treated seawater solution using oxalic acid; Ca^{2+} and Mg^{2+} pre-treated seawater.

4.4. Desorption and regeneration

In this study, HCl was used to desorb/extract Li^+ and regenerate HMO. Different concentrations of HCl ranging from 0.05 M to 1.00 M was used to desorb Li^+ from HMO (Fig. 11a). Close to 96.5 ± 0.8% desorption was achieved with 0.1 M HCl onwards. Based on the results, 0.1 M HCl was selected to extract Li^+ from HMO and for its regeneration. The regenerative/reuse capacity of HMO was evaluated by multiple cycles of adsorbent and desorption (Fig. 8b). In the first cycle, higher Li^+ desorption values than Li^+ uptake occurred, and this could be likely due to Li^+ that was already present in the original HMO. In line with this, Mn dissolution was relatively higher in the first cycle. In the second cycle onwards slightly higher Li^+ uptake occurred and this could be attributed to the higher availability of ion exchange sites due to full Li^+ removal in the first cycle. In the subsequent cycles, Mn dissolution was relatively low and Li^+ uptake was stable with a 7–11% decline in Li^+ uptake rate till the fifth cycle. The results established the feasible regenerative capacity of HMO and likewise, the XRD of the used HMO (Fig. 7) showed minimal damage to its structure. Similar results were reported by previous studies (Shi et al., 2011, Ohashi and Tai, 2019). For instance, Shi et al. analysed the XRD structure of HMO upon 10 cycles of regeneration and indicated its

intact structure, establishing that HMO structure was not significantly affected by repeated cycles of adsorption and desorption. Nevertheless, it must be acknowledged that although regeneration in powder form HMO was possible in a batch study, mass losses will be inevitable in actual scenario. A suitable encapsulation of HMO will thus be necessary to retain its mass and enable a practical application in a dynamic filter column (Park et al., 2014, Naidu et al., 2016).

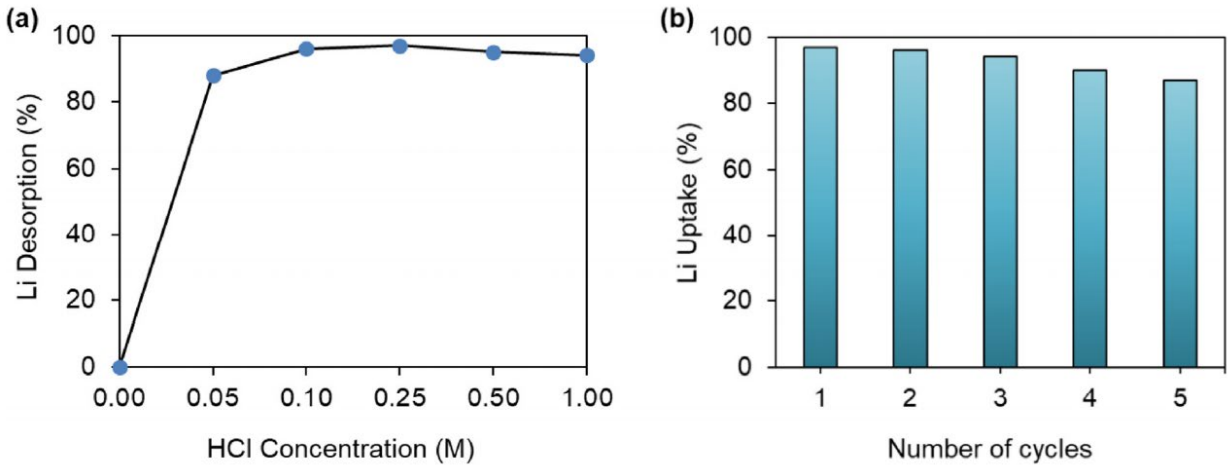

Figure 10: HMO regeneration capacity in terms of (a) Li^+ desorption with HCl at varied concentration (b) Li^+ uptake with 5 cycles of adsorption/desorption with 0.1 M HCl

4.5. Performance of ZIF-8 with H-form manganese oxide (HMO), HMO@ZIF-8

Zeolitic imidazolate metal organic framework (ZIF-8) is a category of microporous MOF containing zinc metal ions with 2-methylimidazole (Hmim) as organic linker (H.N. Abdelhamid 2020, A.F. Abdel-Magied et al 2019 Xue Min et al., 2017). The ZIFs pores predominantly constitute of micro pores that reduces the availability of active sites for ions/molecules adsorption and diffusion into the internal cage of its framework.

Several attempts have been made to produce hierarchical porous ZIF-8 using in-situ and template molecules. In the case of template molecules using organic based molecules, dyes, and enzymes, as well as other template ions/molecules, the tendency is that they tend to occupy the pores formed. As such, additional steps are necessary to remove reagents to gain pore accessibility. However, these steps tend to be in-complete and results in impure residuals in the product. Inevitably, these approaches also lack scalability and is costly as well as time consuming.

The synthesis of hierarchical porous ZIF-8 and a straightforward manner to manipulate the micro/meso-pores has gained much research interest (H.N. Abdelhamid 2020, A.F. Abdel-Magied et al 2019). In this regard, the presence of NaOH has shown to increase the presence of mesopores structure of ZIF-8 (A.F. Abdel-Magied et al.2019) The application of NaOH is advantageous as it is a widely available and cost-effective chemical in comparison to other chemical solvents for instance, ammonia. Further, the synthesis procedure is straightforward as it can be conducted in room temperature in a short span of time and requires mainly water as solvent as opposed to organic solvents (dimethylformamide or methanol). Also, the ZIF-8 product can be attained at ease through filtration without foreseeable residual zinc hydroxides impurities, thereby, eliminating the need for high thermal/temperature, vacuum oven, microwave, and auto thermal synthesis.

The potential of grafting template free ZIF-8 with Li^{+} selective nanoparticle, H-form manganese oxide (HMO), HMO@ZIF-8, to increase its selective adsorption capacity has not been explored to date.

In this study, for the first time a novel synthesis of HMO@ZIF-8 was produced by modifying relevant methods of other studies (Abdelhamid, 2020, Abdel-Magied et al., 2019, Min et al., 2017). The novel method used in this study is shown the Fig 12 and as discussed in detail in Section 3.2.6.2

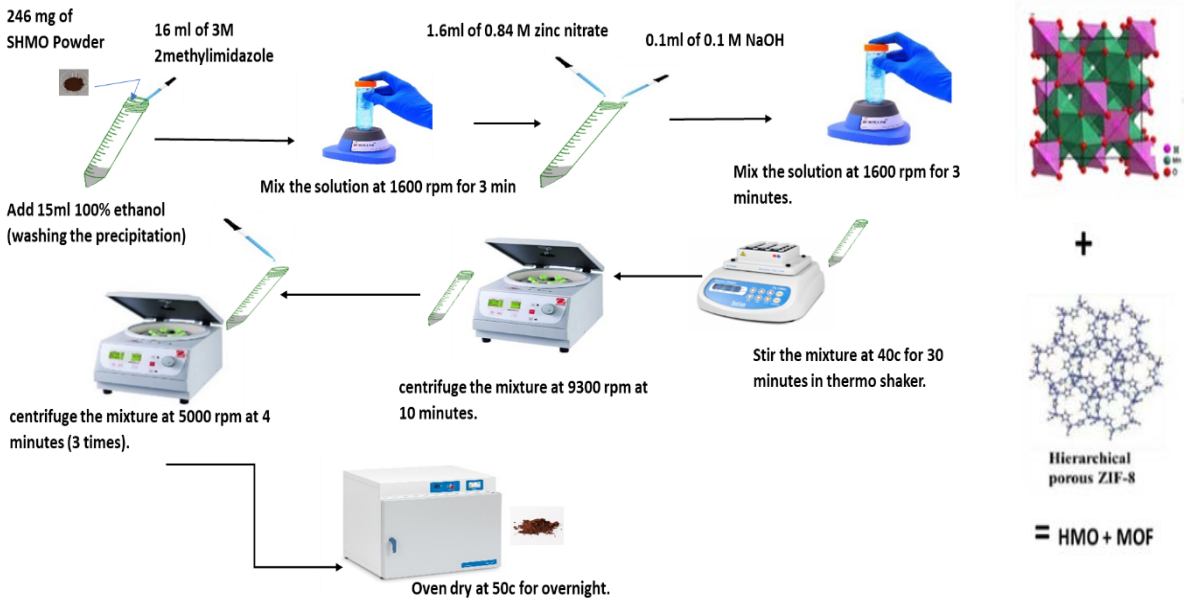

Figure 11: Grafting ZIF-8 with H-form manganese oxide (HMO), HMO@ZIF-8

The results showed that compared to HMO, synthesised HMO@ZIF-8 showed significantly higher adsorption capacity at pH 11 and was able to selectively adsorb Li^+ at pH 8.5 (pH of seawater) as shown in Figure 13. Further in seawater, synthesised HMO@ZIF-8 was able to selectively adsorb Li^+ in pH 8.5 (figure 14).

Based on the results in Figure 13, it was observed that ZIF-8 only (without HMO) showed close to zero Li^+ uptake. The surface area of ZIF-8 as reported by previous studies (A.F. Abdel-Magied et al.2019) is significantly high at over 1000 m^2/g, in comparison to the surface area of HMO which ranges from only 100-150 m^2/g (tian et al., 2010, park et al 2014). Generally, adsorption capacity tends to increase when the surface area of an adsorbent is high. The minimal lithium adsorption with ZIF-8 in spite of its significantly higher surface area compared to HMO, suggest that the mechanism of lithium adsorption is not majorly influenced by physical surface adsorption.

In comparing the performance of HMO and ZIF-8 grafted onto HMO (HMO@ZIF-8), the Li^+ uptake was 89% for HMO@ZIF-8 compared to HMO at pH 11.5. Meanwhile, a significantly higher Li^+ uptake (53%) was attained for HMO@ZIF-8 compared to HMO at pH 8.5. As ZIF-8 only did not result in Li^+ uptake, this indicated that the surface area and surface physical adsorption is not a contributing factor to the higher Li^+ uptake for ZIF-8 grafted onto HMO (HMO@ZIF-8). On another note, the HMO mechanism as described in details in Section 4.3.2., Chapter 4, with regards to the influence of pH and surface zeta charge, established that the high uptake of Li^+ attained at pH above 11.0 was attributed predominantly to the exchange of H with Li^+ due to deprotonation condition at this optimum pH that removed H from the ion sieve, creating vacant site suitable for Li^+ uptake, while at pH 8.5, a much lower uptake occurred, as this optimum condition was not present. However, HMO@ZIF-8 was able to achieve high Li^+ uptake at pH 8.5. These results suggest that the grafting of ZIF-8 onto HMO contributed to a change of Li^+ uptake mechanism. One potential possibility that may have led to the high Li^+ uptake with HMO@ZIF-8 at pH 8.5 was the combined presence of ZIF-8 into HMO that may have influenced the pore cavity size of the adsorbent that enhanced the presence of vacant site suitable for Li^+ uptake. Specifically, the narrow pore size cavities of ZIF-8 in the range of 5-10 Å (Zhang et al., 2018) as reported by previous studies, is a closer match to that of the ionic size of Li (0.76 Å) (as listed in Table 1). Meanwhile the pore size of HMO is significantly higher in the ranges of 900-1000 Å (Park et al, 2016). Hence, the combined presence of ZIF-8 (pore size cavity matching that of Li^+) and HMO (deprotonation between H^+ and Li^+) in

HMO@ZIF-8 may have enabled the exchange of Li^+ with H to occur even at pH 8.5, and thereby, enabling to attain high Li^+ uptake at pH 8.5.

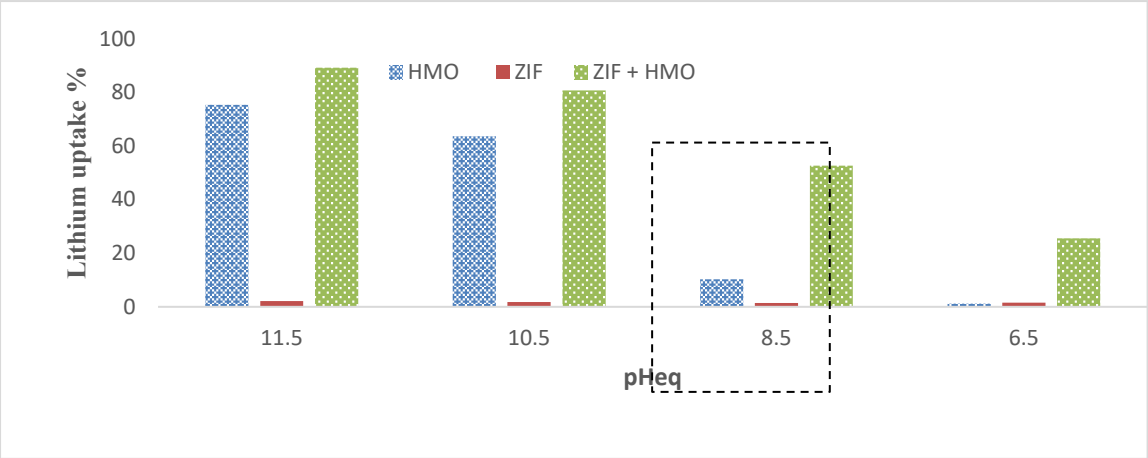

Figure 12:Comparison of lithium uptake by HMO, ZIF-8 and HMO+ZIF-8 in model Li^+ solution (Co = 5 mg Li^+/L; pHeq = 11.5 ± 0.5, 10.5 ± 0.5, 8.5 ± 0.5 and 6.5 ± 0.5; HMO dose = 0.3 g/L).

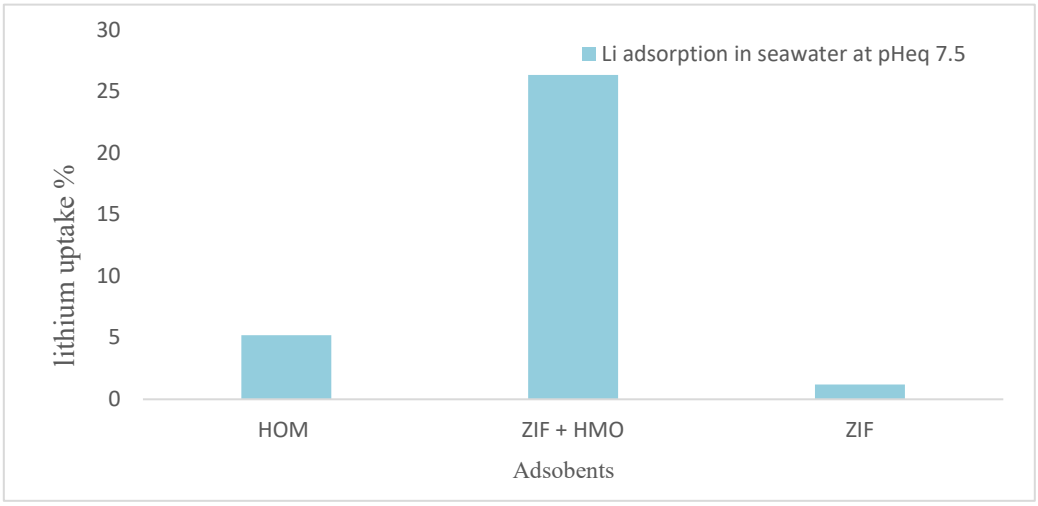

Figure 13: Comparison of ion uptake by HMO, ZIF-8+ HMO, ZIF-8 in, original seawater spiked with Li^+ (Co = 5 Ca Li^+/L; pHeq = 8.5 ± 0.5, HMO dose = 1 g/L).

4.6. Cost Benefit analysis

Table 8: Activities and chemical required to extract lithium from 1 litre of sea water which is approximately (0.17 mg/L).

Activities	**Ingredients**	**Energy and time**	**product**
Ca^{2+} removal using oxalic acid	Seawater Oxalic acid (2g)	Magnetic Stirring (24h) Filtering (1h)	Pre-treated seawater 0.53g calcium oxide 4.42g sodium hydroxide
Organic Removal	Granular activated carbon (50g)	Magnetic Stirring (24h) Filtering (1h)	Organic reduced pre-treated seawater
Membrane distillation	Organic reduced pre-treated seawater, Membrane, Citric acid (10g)	Cooling at 8C/ 36h, Heating at 55C, Magnetic Stirrer, Circulating water flow	Good quality water Concentrated brine
Mg^{2+} Removal	Sodium hydroxide (1.5g)	Magnetic stirring (48h) Filtering (2h)	2g of magnesium divalent removed concentrated seawater.
HMO absorbent preparation	4g manganese oxide 5.55g Lithium hydroxide 100ml 37% HCl	Stirring (1h), Autoclave at 120^0C (24h), Centrifuge (1h), Oven dry 60◦C (12h), heating 400◦C (4h), stirring (12h), filtering (5h), Oven dry 50◦C (12h)	4g HMO adsorbent
Adsorption	Seawater brine (0.17 mg Li^+) (140ml)	Stirring (24h), Filtering (10 min)	4g ~ LMO

	HMO (0.5g), NaOH pinch		
Activities	**Ingredients**	**Energy and time**	**Product**
Desorption	4g ~ LMO, HCL (12ml)	Stirring (24h) Filtering (10 min)	HMO 0.5g 0.58mg Lithium chloride
MOF absorbent preparation	246g HMO powder 4g 2-methylimidazole, 400mg zing nitrate, 10mg sodium hydroxide	Centrifuge 9300rpm 30min), Stirring 40◦C (30min), Oven dry 50◦C (21h), Mix the solution (6min)	HMO@ZIF-8
Adsorption	HMO@ZIF-8 (1g) Seawater brine (140 ml)	Stirring (24h), Filtering (10 min)	LMO@ZIF-8

Li^+ recovery is main target in this analysis. While it is processed, it also produces by-products such as treated water, magnesium hydroxide, calcium oxide and sodium hydroxide. As this is a initial lab scale study, it is very difficult to quantitatively estimate the cost and benefits of this process. Therefore, a matrix of cost and socio-economic benefit is presented for the following 2 processes in terms of energy demand, degree of automation, Capex, Opex, and ecological impact

Process 1: Calcium removal+ Organic removal + Membrane distillation + Magnesium removal + HMO Preparation + Adsorption + Desorption.

Process 2: Calcium removal+ Organic removal + Membrane distillation + Magnesium removal + HMO@MOF + Adsorption

4.6.1. Energy demand

The amount of energy consumed per gram of Lithium extracted is expressed in kWh/g.The energy demand is assessed as high, medium and low based on the following scoring scale.

Table 9: Energy demand - *scores*

Level	High	> 100 kWh/g
	Medium	10 < x ≤ 100 kWh/g
	Low	0.1 < x ≤ 10 kWh/g

4.6.2. Degree of automation

The quantity assessed is the amount of labour that is needed for operation and maintenance. This addresses only the quantity of work and thus the degree of automation; and in no respect it reflects the quality of work.

Table 10. Degree of automation - scores

Level	Low	Several full-time workers
	Medium	One full-time worker
	High	One part-time worker

4.6.3. CAPEX

The capital expenditure (CAPEX) includes the cost of equipment, construction, and installations for each unit process in a treatment train configuration, the cost of energy required for construction and installation and the cost of land required. CAPEX is related to the amount of Lithium extracted during the whole life span and thus expressed as $/g.

Table 11. CAPEX - scores

Level	High	> 100 $/g)
	Medium	10 < x ≤ 100 $/g
	Low	0 < x ≤ 10 $/g

4.6.4. OPEX

Operational expenditure (OPEX) comprises of the cost of energy required to run the treatment system (e.g. pumping), the cost of labour required, the cost of disposal of waste by-products (e.g. sludge), the cost of chemicals required for treatment, and the cost of monitoring,

maintenance and repairs including cost of spare parts. OPEX is related to the amount of water produced during the whole life span and thus expressed as $/g.

Table 11. OPEX - scores

Level	High	> 100 $/g
	Medium	10 < x ≤ 100 $/g
	Low	1 < x ≤ 10 $/g

4.6.5. Ecological impact (of by-products)

The impact on the environment on the disposal of by-products or waste (i.e Ecological impact) was also assessed based on the following scores. They may be toxic or have negative effect on the environment. Also, emission of toxic materials to environment in the case of a major accident should be considered.

Table 12. Ecologic impact - scores

Level	High	Toxic waste
	Medium	Non-toxic waste
	Low	No waste generated

4.6.6. Process train

Process train	**Energy demand**	**Degree of automation**	**CAPEX**	**OPEX**	**Ecologic impact (of by-products)**
Process 1	High	Medium	High	High	Medium
Process 2	High	Medium	High	High	Medium

CHAPTER 5

CONCLUSION AND RECOMMENDATIONS

5. Conclusion and Recommendations.

In this final chapter the main outcomes of this work are summarized and recommendations for the potential of recovering Li^+ from concentrate seawater are given.

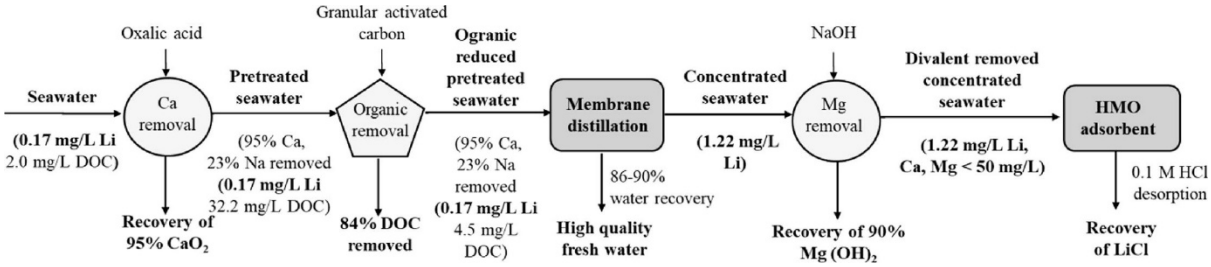

Figure 14. stoichiometric diagram of the overall study.

5.1 Conclusion

The focus of this study was to enhance the recovery of water and Li^+ in seawater. For these reasons, the study evaluated (i) the suitability of oxalic acid as a seawater chemical softening treatment; (ii) water recovery rate of DCMD with pre-treated seawater; and (iii) the capacity of HMO for selective Li^+ uptake from concentrated seawater. The results of this study established that:

a. Oxalic acid was highly suitable as a seawater chemical treatment for removing over 95% of Ca^{2+} from seawater without any additional ion residues. Comparatively, caustic soda ash approach removed Ca^{2+} simultaneously with Mg^{2+}, while increasing Na content in seawater.

b. The addition of oxalic acid into seawater significantly increased its organic content. A simple approach of granular activated carbon adsorption was effective to reduce the organic content in oxalic acid treated seawater by 84%.

c. DCMD was able to concentrate oxalic acid treated seawater by up to volume concentration factor (VCF) of 7.5. This was attributed to reduced ion concentration and delayed induction of ion precipitation in acidic condition with oxalic acid treatment. Comparatively, DCMD operation with caustic soda ash treated seawater only achieve a VCF of 3.7 before experiencing flux decline.

d. DCMD process enabled to produce fresh water (86% water recovery) from oxalic acid treated seawater while successfully increasing Li^+ concentration by 7–8 times (0.17 mg/L to 1.22 mg/L).

e. HMO adsorbent exhibited favourable capacity for Li^+ uptake attributed to selective H^+/Li^+ exchange in alkaline condition, enabling to achieve a Langmuir Q_{max} of 17.8 mg/g.

f. The presence of Mg^{2+} in seawater was the main ion competitor that reduced Li^+ uptake in seawater, attributed to the closely similar ionic radii of Li^+ and Mg^{2+} and the high electronegativity of Mg^{2+} compared to Li^+. Upon Mg^{2+} removal, HMO was able to maintain high selective Li^+ uptake from seawater.

g. It is not possible to achieve resource recovery by a single process. The treatment process in stages – pre-treating, removing divalent and concentrating seawater, followed by adsorption by HMO, provides a favourable scenario for attaining high selective Li^+ recovery from seawater as well as for recovering fresh water and other valuable products – Ca^{2+} and Mg^{2+}.

h. In comparison to conventional HMO, the newly synthesised HMO with metal organic framework -ZIF-8@HMO, showed higher Li^+ adsorption capacity. More importantly, ZIF-8@HMO is able to selectively extract Li^+ in seawater at its original pH (7.5-8.0). This is favourable in attaining selectively Li^+ recovery from seawater without the need for chemical addition (NaOH) for pH change to 11.

5.2. Recommendations

The results of this study showed the promising capacity to concentrate seawater and recovery Li $^+$using membrane distillation and ZIF-8@HMO, and therefore it is recommended that this potential method can be adopted in a desalination plant for recovering Li^+. However, it is important to test this concept in a pilot scale system and for a detail techno-economic analysis to be carried out to evaluate the cost saving measure that could be attained by a desalination plant. Likewise, compared to HMO, the high Li^+ selective capacity of ZIF-8@HMO is promising and therefore, it is recommended to explore more types of ZIF-8@HMO synthesis method to further enhance the selective Li^+ recovery capacity from seawater.

Reference

ABDEL-MAGIED, A. F., ABDELHAMID, H. N., ASHOUR, R. M., ZOU, X. & FORSBERG, K. 2019. Hierarchical porous zeolitic imidazolate frameworks nanoparticles for efficient adsorption of rare-earth elements. Microporous and Mesoporous Materials, 278, 175-184.

ABDELHAMID, H. N. 2020. Zinc hydroxide nitrate nanosheets conversion into hierarchical zeolitic imidazolate frameworks nanocomposite and their application for CO2 sorption. Materials Today Chemistry, 15, 100222.

ALSABAH, H., BERNARD, B., CAPPONI, A., IYENGAR, G. & SETHURAMAN, J. Multiregional Oligopoly with Capacity Constraints. Management Science, 0, null.

BHATNAGAR, A. & SILLANPÄÄ, M. 2010. Utilization of agro-industrial and municipal waste materials as potential adsorbents for water treatment—A review. Chemical Engineering Journal, 157, 277-296.

BROUWER, A. S., VAN DEN BROEK, M., ZAPPA, W., TURKENBURG, W. C. & FAAIJ, A. 2016. Least-cost options for integrating intermittent renewables in low-carbon power systems. Applied Energy, 161, 48-74.

CASTILLO, E. H. C., THOMAS, N., AL-KETAN, O., ROWSHAN, R., ABU AL-RUB, R. K., NGHIEM, L. D., VIGNESWARAN, S., ARAFAT, H. A. & NAIDU, G. 2019. 3D printed spacers for organic fouling mitigation in membrane distillation. Journal of Membrane Science, 581, 331-343.

CHEN, N., TAO, S., XIAO, K., LIANG, S., YANG, J. & ZHANG, L. 2020. A one-step acidification strategy for sewage sludge dewatering with oxalic acid. Chemosphere, 238, 124598.

CHITRAKAR, R., KANOH, H., MIYAI, Y. & OOI, K. 2001. Recovery of Lithium from Seawater Using Manganese Oxide Adsorbent (H1.6Mn1.6O4) Derived from Li1.6Mn1.6O4. Industrial & Engineering Chemistry Research, 40, 2054-2058.

CHOI, J., DORJI, P., SHON, H. K. & HONG, S. 2019. Applications of capacitive deionization: Desalination, softening, selective removal, and energy efficiency. Desalination, 449, 118-130.

CHOI, Y., NAIDU, G., JEONG, S., VIGNESWARAN, S., LEE, S., WANG, R. & FANE, A. G. 2017. Experimental comparison of submerged membrane distillation configurations for concentrated brine treatment. Desalination, 420, 54-62.

CHOUBEY, P. K., KIM, M.-S., SRIVASTAVA, R. R., LEE, J.-C. & LEE, J.-Y. 2016. Advance review on the exploitation of the prominent energy-storage element: Lithium. Part I: From mineral and brine resources. Minerals Engineering, 89, 119-137.

CRISCUOLI, A., BAFARO, P. & DRIOLI, E. 2013. Vacuum membrane distillation for purifying waters containing arsenic. Desalination, 323, 17-21.

DABROWSKI, A. 2001. Adsorption--from theory to practice. Adv Colloid Interface Sci, 93, 135-224.

EL-BOURAWI, M. S., DING, Z., MA, R. & KHAYET, M. 2006. A framework for better understanding membrane distillation separation process. Journal of Membrane Science, 285, 4-29.

EYKENS, L., HITSOV, I., DE SITTER, K., DOTREMONT, C., PINOY, L., NOPENS, I. & VAN DER BRUGGEN, B. 2016. Influence of membrane thickness and process conditions on direct contact membrane distillation at different salinities. Journal of Membrane Science, 498, 353-364.

FENG, Q., MIYAI, Y., KANOH, H. & OOI, K. 1992. Lithium(1+) extraction/insertion with spinel-type lithium manganese oxides. Characterization of redox-type and ion-exchange-type sites. Langmuir, 8, 1861-1867.

FLEXER, V., BASPINEIRO, C. F. & GALLI, C. I. 2018. Lithium recovery from brines: A vital raw material for green energies with a potential environmental impact in its mining and processing. Science of The Total Environment, 639, 1188-1204.

GLÖSER, S., TERCERO ESPINOZA, L., GANDENBERGER, C. & FAULSTICH, M. 2015. Raw material criticality in the context of classical risk assessment. Resources Policy, 44, 35-46.

GONZÁLEZ, D., AMIGO, J. & SUÁREZ, F. 2017. Membrane distillation: Perspectives for sustainable and improved desalination. Renewable and Sustainable Energy Reviews, 80, 238-259.

GRANATA, G., MOSCARDINI, E., PAGNANELLI, F., TRABUCCO, F. & TORO, L. 2012. Product recovery from Li-ion battery wastes coming from an industrial pre-treatment plant: Lab scale tests and process simulations. Journal of Power Sources, 206, 393-401.

GREGSON, N., CRANG, M., FULLER, S. & HOLMES, H. 2015. Interrogating the circular economy: the moral economy of resource recovery in the EU. Economy and Society, 44, 218-243.

GROSJEAN, C., MIRANDA, P. H., PERRIN, M. & POGGI, P. 2012. Assessment of world lithium resources and consequences of their geographic distribution on the expected development of the electric vehicle industry. Renewable and Sustainable Energy Reviews, 16, 1735-1744.

GRUBER, P. W., MEDINA, P. A., KEOLEIAN, G. A., KESLER, S. E., EVERSON, M. P. & WALLINGTON, T. J. 2011. Global Lithium Availability. Journal of Industrial Ecology, 15, 760-775.

GRYTA, M. 2010. Desalination of thermally softened water by membrane distillation process. Desalination, 257, 30-35.

GU, D., SUN, W., HAN, G., CUI, Q. & WANG, H. 2018. Lithium ion sieve synthesized via an improved solid state method and adsorption performance for West Taijinar Salt Lake brine. Chemical Engineering Journal, 350, 474-483.

GUAN, G., YAO, C., LU, S., JIANG, Y., YU, H. & YANG, X. 2018. Sustainable operation of membrane distillation for hypersaline applications: Roles of brine salinity, membrane permeability and hydrodynamics. Desalination, 445, 123-137.

GUEST, J. S., SKERLOS, S. J., BARNARD, J. L., BECK, M. B., DAIGGER, G. T., HILGER, H., JACKSON, S. J., KARVAZY, K., KELLY, L., MACPHERSON, L., MIHELCIC, J. R., PRAMANIK, A., RASKIN, L., LOOSDRECHT, M. C. M. V., YEH, D. & LOVE, N. G. 2009. A new planning and design paradigm to achieve sustainable resource recovery from wastewater. Environmental Science & Technology, 43, 6126-6130.

HAN, Y., KIM, H. & PARK, J. 2012. Millimeter-sized spherical ion-sieve foams with hierarchical pore structure for recovery of lithium from seawater. Chemical Engineering Journal, 210, 482-489.

HERALD, S. M. 2018. Australia tipped to soon produce more than half of the world's lithium. Sydney Morning Herald

HITSOV, I., MAERE, T., DE SITTER, K., DOTREMONT, C. & NOPENS, I. 2015. Modelling approaches in membrane distillation: A critical review. Separation and Purification Technology, 142, 48-64.

HOLDREN, J. P. 1971. Adequacy of lithium supplies as a fusion energy source. ; California Univ., Livermore (USA). Lawrence Livermore Lab.

HONG, H.-J., PARK, I.-S., RYU, T., KIM, B.-G. & CHUNG, K.-S. 2019. Macroporous Hydrogen Manganese Oxide/Al2O3 for Effective Lithium Recovery from Seawater: Effects of the Macropores vs Mesopores. Industrial & Engineering Chemistry Research, 58, 8342-8348.

HONG, H.-J., PARK, I.-S., RYU, T., RYU, J., KIM, B.-G. & CHUNG, K.-S. 2013. Granulation of Li1.33Mn1.67O4 (LMO) through the use of cross-linked chitosan for the effective recovery of Li+ from seawater. Chemical Engineering Journal, 234, 16-22.

HORNE, R. N. 1982. GEOTHERMAL REINJECTION EXPERIENCE IN JAPAN. JPT, Journal of Petroleum Technology, 34, 495-503.

JI, X., CURCIO, E., AL OBAIDANI, S., DI PROFIO, G., FONTANANOVA, E. & DRIOLI, E. 2010. Membrane distillation-crystallization of seawater reverse osmosis brines. Separation and Purification Technology, 71, 76-82.

KHAYET, M. 2011. Membranes and theoretical modeling of membrane distillation: A review. Advances in Colloid and Interface Science, 164, 56-88.

KIM, H.-W., YUN, T., HONG, S., LEE, S. & JEONG, S. 2020. Retardation of wetting for membrane distillation by adjusting major components of seawater. Water Research, 175, 115677.

KNOSHAUG, E. P., DONG, T., SPILLER, R., NAGLE, N. & PIENKOS, P. T. 2018. Pretreatment and fermentation of salt-water grown algal biomass as a feedstock for biofuels and high-value biochemicals. Algal Research, 36, 239-248.

LALASARI, L., ANDRIYAH, L., ARINI, T., SULISTIYONO, E., PRASETYO, A. B., FIRDIYONO, F. & NATASHA, N. 2020. Lithium extraction from brine water Tirtasanita Bogor, Indonesia by evaporation method. Journal of Physics: Conference Series, 1450, 012013.

LALASARI, L., FATAHILLAH, F., RAHMAT, D., TARMIZI, E., RHAMDANI, A., SULISTIYONO, E., ANDRIYAH, L., ARINI, T., NATASHA, N. & FIRDIYONO, F. 2019.

Magnesium removal from brine water with low lithium grade using limestone, rembang, indonesia. IOP Conference Series: Materials Science and Engineering, 578, 012067.

LAWSON, K. W. & LLOYD, D. R. 1996. Membrane distillation. II. Direct contact MD. Journal of Membrane Science, 120, 123-133.

LEE, H.-J., SEO, Y.-J. & LEE, J.-W. 2013. Characterization of oxalic acid pretreatment on lignocellulosic biomass using oxalic acid recovered by electrodialysis. Bioresource Technology, 133, 87-91.

LEE, J.-G., JANG, Y., FORTUNATO, L., JEONG, S., LEE, S., LEIKNES, T. & GHAFFOUR, N. 2018. An advanced online monitoring approach to study the scaling behavior in direct contact membrane distillation. Journal of Membrane Science, 546, 50-60.

LI, N., LU, D., ZHANG, J. & WANG, L. 2018. Yolk-shell structured composite for fast and selective lithium ion sieving. J Colloid Interface Sci, 520, 33-40.

LI, X., MO, Y., QING, W., SHAO, S., TANG, C. Y. & LI, J. 2019. Membrane-based technologies for lithium recovery from water lithium resources: A review. Journal of Membrane Science, 591, 117317.

LIANG, Q., ZHANG, E.-H., YAN, G., YANG, Y.-Z., LIU, W.-F. & LIU, X.-G. 2020. A lithium ion-imprinted adsorbent using magnetic carbon nanospheres as a support for the selective recovery of lithium ions. New Carbon Materials, 35, 696-706.

LIU, L., ZHANG, H., ZHANG, Y., CAO, D. & ZHAO, X. 2015. Lithium extraction from seawater by manganese oxide ion sieve MnO2·0.5H2O. Colloids and Surfaces A: Physicochemical and Engineering Aspects, 468, 280-284.

LOGANATHAN, P., NAIDU, G. & VIGNESWARAN, S. 2017. Mining valuable minerals from seawater: a critical review. Environmental Science: Water Research & Technology, 3, 37-53.

LUO, X., ZHANG, K., LUO, J., LUO, S. & CRITTENDEN, J. 2016. Capturing Lithium from Wastewater Using a Fixed Bed Packed with 3-D MnO2 Ion Cages. Environmental Science & Technology, 50, 13002-13012.

MERICQ, J.-P., LABORIE, S. & CABASSUD, C. 2010. Vacuum membrane distillation of seawater reverse osmosis brines. Water Research, 44, 5260-5273.

MESHRAM, P., PANDEY, B. D. & MANKHAND, T. R. 2014. Extraction of lithium from primary and secondary sources by pre-treatment, leaching and separation: A comprehensive review. Hydrometallurgy, 150, 192-208.

MIN, X., YANG, W., GAO, C., DANG, S., HUI, Y.-F. & SUN, Z.-M. 2017. Fe3O4@ZIF-8: A Magnetic Nanocomposite for Highly Efficient UO2(2+) Adsorption and Selective UO2(2+)/Ln(3+) Separation. Chem. Commun., 53.

MOLDOVEANU, G. A. & PAPANGELAKIS, V. G. 2015. Strategies for calcium sulphate scale control in hydrometallurgical processes at 80°C. Hydrometallurgy, 157, 133-139.

NAIDU, G., JEONG, S., CHOI, Y., SONG, M. H., OYUNCHULUUN, U. & VIGNESWARAN, S. 2018. Valuable rubidium extraction from potassium reduced seawater brine. Journal of Cleaner Production, 174, 1079-1088.

NAIDU, G., JEONG, S., CHOI, Y. & VIGNESWARAN, S. 2017. Membrane distillation for wastewater reverse osmosis concentrate treatment with water reuse potential. Journal of Membrane Science, 524, 565-575.

NAIDU, G., JEONG, S. & VIGNESWARAN, S. 2015. Interaction of humic substances on fouling in membrane distillation for seawater desalination. Chemical Engineering Journal, 262, 946-957.

NAIDU, G., LOGANATHAN, P., JEONG, S., JOHIR, M. A. H., TO, V. H. P., KANDASAMY, J. & VIGNESWARAN, S. 2016. Rubidium extraction using an organic polymer encapsulated potassium copper hexacyanoferrate sorbent. Chemical Engineering Journal, 306, 31-42.

NAIDU, G., TIJING, L., JOHIR, M. A. H., SHON, H. & VIGNESWARAN, S. 2020. Hybrid membrane distillation: Resource, nutrient and energy recovery. Journal of Membrane Science, 599, 117832.

NISHIHAMA, S., ONISHI, K. & YOSHIZUKA, K. 2011. Selective Recovery Process of Lithium from Seawater Using Integrated Ion Exchange Methods. Solvent Extraction and Ion Exchange, 29, 421-431.

OBER, J. A. 2018. Mineral commodity summaries 2018. Mineral Commodity Summaries. Reston, VA.

OHASHI, F. & TAI, Y. 2019. Lithium adsorption from natural brine using surface-modified manganese oxide adsorbents. Materials Letters, 251, 214-217.

OPITZ, A., BADAMI, P., SHEN, L., VIGNAROOBAN, K. & KANNAN, A. M. 2017. Can Li-Ion batteries be the panacea for automotive applications? Renewable and Sustainable Energy Reviews, 68, 685-692.

PARK, M. J., NISOLA, G. M., BELTRAN, A. B., TORREJOS, R. E. C., SEO, J. G., LEE, S.-P., KIM, H. & CHUNG, W.-J. 2014. Recyclable composite nanofiber adsorbent for Li+ recovery from seawater desalination retentate. Chemical Engineering Journal, 254, 73-81.

QU, D., WANG, J., WANG, L., HOU, D., LUAN, Z. & WANG, B. 2009. Integration of accelerated precipitation softening with membrane distillation for high-recovery desalination of primary reverse osmosis concentrate. Separation and Purification Technology, 67, 21-25.

RAZMJOU, A., ASADNIA, M., HOSSEINI, E., HABIBNEJAD KORAYEM, A. & CHEN, V. 2019. Design principles of ion selective nanostructured membranes for the extraction of lithium ions. Nature Communications, 10, 5793.

RYU, T., HALDORAI, Y., RENGARAJ, A., SHIN, J., HONG, H.-J., LEE, G.-W., HAN, Y.-K., HUH, Y. S. & CHUNG, K.-S. 2016. Recovery of Lithium Ions from Seawater Using a Continuous Flow Adsorption Column Packed with Granulated Chitosan–Lithium Manganese Oxide. Industrial & Engineering Chemistry Research, 55, 7218-7225.

RYU, T., SHIN, J., GHOREISHIAN, S. M., CHUNG, K.-S. & HUH, Y. S. 2019. Recovery of lithium in seawater using a titanium intercalated lithium manganese oxide composite. Hydrometallurgy, 184, 22-28.

SALMANI NURI, O., IRANNAJAD, M. & MEHDILO, A. 2019. Effect of surface dissolution by oxalic acid on flotation behavior of minerals. Journal of Materials Research and Technology, 8, 2336-2349.

SANMARTINO, J. A., KHAYET, M., GARCÍA-PAYO, M. C., EL-BAKOURI, H. & RIAZA, A. 2017. Treatment of reverse osmosis brine by direct contact membrane distillation: Chemical pretreatment approach. Desalination, 420, 79-90.

SEMBLANTE, G. U., LEE, J. Z., LEE, L. Y., ONG, S. L. & NG, H. Y. 2018. Brine pre-treatment technologies for zero liquid discharge systems. Desalination, 441, 96-111.

SHAHMANSOURI, A., MIN, J., JIN, L. & BELLONA, C. 2015. Feasibility of extracting valuable minerals from desalination concentrate: a comprehensive literature review. Journal of Cleaner Production, 100, 4-16.

SHI, C., DUAN, D., JIA, Y. & JING, Y. 2014. A highly efficient solvent system containing ionic liquid in tributyl phosphate for lithium ion extraction. Journal of Molecular Liquids, 200, 191-195.

SHI, X., ZHOU, D., ZHANG, Z., YU, L., XU, H., CHEN, B. & YANG, X. 2011. Synthesis and properties of Li1.6Mn1.6O4 and its adsorption application. Hydrometallurgy, 110, 99-106.

SIEKIERKA, A., TOMASZEWSKA, B. & BRYJAK, M. 2018. Lithium capturing from geothermal water by hybrid capacitive deionization. Desalination, 436, 8-14.

SONG, J. F., NGHIEM, L. D., LI, X.-M. & HE, T. 2017. Lithium extraction from Chinese salt-lake brines: opportunities, challenges, and future outlook. Environmental Science: Water Research & Technology, 3, 593-597.

SOROUR, M. H., HANI, H. A., SHAALAN, H. F. & AL-BAZEDI, G. A. 2015. Schemes for salt recovery from seawater and RO brines using chemical precipitation. Desalination and Water Treatment, 55, 2398-2407.

SURVEY, U. S. G. 2018. U.S. Geological Survey

TIAN, L., MA, W. & HAN, M. 2010. Adsorption behavior of Li+ onto nano-lithium ion sieve from hybrid magnesium/lithium manganese oxide. Chemical Engineering Journal, 156, 134-140.

W.A. HART, O. F. B. 1973. The Chemistry of Lithium Sodium Potassium Cesium and Francium, Inorganic Chemistry, New York, USA,, Pergmum Press

WANG, H., CUI, J., LI, M., GUO, Y., DENG, T. & YU, X. 2020. Selective recovery of lithium from geothermal water by EGDE cross-linked spherical CTS/LMO. Chemical Engineering Journal, 389, 124410.

WANG, J., CHEN, M., CHEN, H., LUO, T. & XU, Z. 2012. Leaching Study of Spent Li-ion Batteries. Procedia Environmental Sciences, 16, 443-450.

WANG, S., CHEN, X., ZHANG, Y., ZHANG, Y. & ZHENG, S. 2018a. Lithium adsorption from brine by iron-doped titanium lithium ion sieves. Particuology, 41, 40-47.

WANG, S., ZHENG, S., WANG, Z., CUI, W., ZHANG, H., YANG, L., ZHANG, Y. & LI, P. 2018b. Superior lithium adsorption and required magnetic separation behavior of iron-doped lithium ion-sieves. Chemical Engineering Journal, 332, 160-168.

WENG, D., DUAN, H., HOU, Y., HUO, J., CHEN, L., ZHANG, F. & WANG, J. 2020. Introduction of manganese based lithium-ion Sieve-A review. Progress in Natural Science: Materials International, 30, 139-152.

WINTER, D., KOSCHIKOWSKI, J. & WIEGHAUS, M. 2011. Desalination using membrane distillation: Experimental studies on full scale spiral wound modules. Journal of Membrane Science, 375, 104-112.

WINTER, M. & BRODD, R. J. 2004. What are batteries, fuel cells, and supercapacitors? Chemical Reviews, 104, 4245-4269.

XIAO, J., NIE, X., SUN, S., SONG, X., LI, P. & YU, J. 2015. Lithium ion adsorption–desorption properties on spinel Li4Mn5O12 and pH-dependent ion-exchange model. Advanced Powder Technology, 26, 589-594.

ZANTE, G., BOLTOEVA, M., MASMOUDI, A., BARILLON, R. & TRÉBOUET, D. 2019. Lithium extraction from complex aqueous solutions using supported ionic liquid membranes. Journal of Membrane Science, 580, 62-76.

ZHANG, H.-Z., XU, Z.-L., DING, H. & TANG, Y.-J. 2017. Positively charged capillary nanofiltration membrane with high rejection for Mg^{2+} and Ca^{2+} and good separation for Mg^{2+} and Li^{+}. Desalination, 420, 158-166.

ZHANG, H., HOU, J., HU, Y., WANG, P., OU, R., JIANG, L., LIU, J. Z., FREEMAN, B. D., HILL, A. J. & WANG, H. 2018. Ultrafast selective transport of alkali metal ions in metal organic frameworks with subnanometer pores. Sci Adv, 4, eaaq0066.

ZHANG, Q.-H., LI, S.-P., SUN, S.-Y., YIN, X.-S. & YU, J.-G. 2009. Lithium selective adsorption on 1-D MnO2 nanostructure ion-sieve. Advanced Powder Technology, 20, 432-437.

Zhang, X., Zhao, W., Zhang, Y. & Jegatheesan, V. 2021, 'A review of resource recovery from seawater desalination brine', Reviews in Environmental Science and Bio/Technology, vol. 20, no. 2, pp. 333-61.